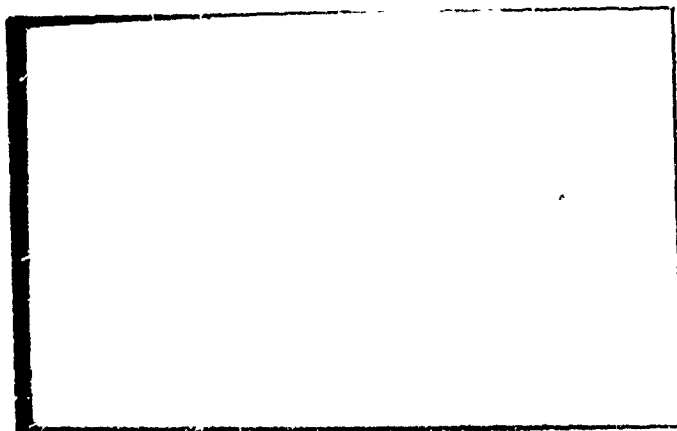
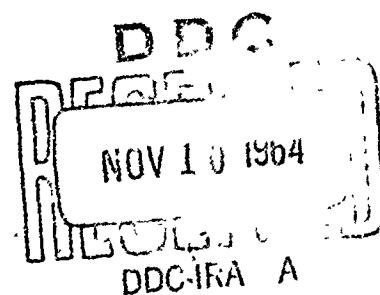


AD 607887



COPY	2	3	10
HARD COPY		\$3.00	
MICROFILM		\$0.75	

60p



ARCHIVE COPY

ELECTRICAL ENGINEERING RESEARCH LABORATORY
ENGINEERING EXPERIMENT STATION
UNIVERSITY OF ILLINOIS
URBANA, ILLINOIS

A WIDEBAND VERTICAL INCIDENCE
RADIO LOCATION ARRAY

September, 1964

RRL Publication No. 259 ✓

by

Fred Ore

Technical Report No. 7 ✓

Contract 89229 ✓

Supported by

BUREAU OF SHIPS

RADIOLOCATION RESEARCH LABORATORY
DEPARTMENT OF ELECTRICAL ENGINEERING
ENGINEERING EXPERIMENT STATION
UNIVERSITY OF ILLINOIS
URBANA, ILLINOIS

Edgar C. Hayden
E. C. Hayden

P. E. Mayes
P. E. Mayes

TABLE OF CONTENTS

	Page
1. Introduction	1
2. General Approach To The Design Of The Vertical Incidence D/F Array	1
3. Small Model Pattern Investigation	7
4. Pattern Calculations	20
5. Impedance Measurements	26
6. Conclusion	50

ILLUSTRATIONS

<u>Figure</u>		<u>Page</u>
1.	(a) Pictorial View of the Radiation Pattern of a 4-Element Array Operating in the Difference Mode. (b) Pictorial View of the Radiation Pattern of a 4-Element Array in the Sum Mode. (c) Desired Beamwidth of the Sum Mode and Beam Location of the Difference Mode.	2
2.	Log-Periodic Dipole Array.	4
3.	Two Element Log-Periodic Dipole Array Over Ground.	5
4.	Four Log-Periodic Dipole Array Elements Forming the Four Sides of an Inverted Pyramid Positioned Over Ground.	6
5a.	Representative Dimensions of a Full Scale 2-Element Vertical Incidence Array Designed for the 2-32 Mc Frequency Range.	8
5b.	Representative Dimensions of a Full Scale 2 Element Vertical Incidence Array Designed for the 2-32 Mc Frequency Range.	9
6.	(a) General Contruction of a Single Log-Periodic Dipole Array Element Used for Pattern Measurements. (b) Typical Feed Point of a 2-Element Array Pattern Model	12
7.	Representative Sum and Difference Patterns of a Two Element Array.	13
8.	The Measured Angle From the Zenith of the Difference Lobes as a Function of ψ Angle for Several Pattern Models Listed in Table I.	14
9.	The Measured Angle From the Zenith of the Difference Lobes as a Function of α Angle for Several Pattern Models of Table I.	15
10.	High Frequency Log-Periodic Dipole-Array Element Model.	17
11.	Representative Free Space Patterns of the Single Element High-Frequency Dipole Array Model.	18
12.	Representative Sum and Difference Patterns of the High Frequency Model of a Two Element Vertical Incidence Array.	19
13.	Diagram of a 2-Element Vertical Incidence Array Over Perfect Ground and Formula Used to Calculate Sum or Difference Patterns for this Array.	22
14.	Location of Phase Center from the Vertex of a Log-Periodic Dipole Array in Terms of Wavelength as a Function of α Angle.	23
15.	Calculated Sum and Difference Patterns of the Two Element Log-Periodic Vertical Incidence Array.	24
16.	Calculated Sum and Difference Patterns of the Two Element Log-Periodic Vertical Incidence Array.	25

Illustrations continued --

<u>Figure</u>		<u>Page</u>
17.	Measured and Calculated Difference Mode Beam Location from the Zenith as a Function of ψ Angle.	27
18.	Calculated Sum and Difference Patterns of the Two Element Log-Periodic Vertical Incidence Array.	28
19.	Calculated Sum and Difference Patterns of the Two Element Log-Periodic Vertical Incidence Array.	29
20.	Measured and Calculated Difference Mode Beam Location from the Zenith as a Function of ψ Angle.	30
21.	Calculated and Measured Sum Mode Beamwidths as a Function of ψ Angle.	31
22.	Free Space Input Impedance and VSWR of a Two Element Array Connected in a Sum or Difference Mode.	33
23.	Free Space Input Impedance and VSWR of a Two Element Array Connected in a Sum or Difference Mode.	34
24.	VSWR and Input Impedance as a Function of Angle Above Ground, $\beta/2$, for Various α Angles.	35
25.	Construction Techniques Used for Impedance and Pattern Models.	37
26.	VSWR and Input Impedance as a Function of Angle Above Ground, $\beta/2$, for Various α Angles.	39
27.	Free Space VSWR and Input Impedance as a Function of α Angle.	40
28.	A Sketch of the Impedance Model Having the Spiral Open Wire Feeder Line.	42
29.	Feed Techniques Used on Low Frequency Impedance Models.	44
30.	Comparison of the Input Impedance of a Single Log-Periodic Dipole Array Element Over Ground, Fed at the Vertex (a) Without a Transformer (b) With a Transformer	46
31.	VSWR and Input Impedance as a Function of Angle Above Ground, $\beta/2$, for Various α Angles.	47
32.	VSWR and Input Impedance as a Function of $\beta/2$ in Degrees for Sum and Difference Modes.	48
33.	VSWR and Input Impedance as a Function of $b/2$ in Degrees for Sum and Difference Modes.	49

ACKNOWLEDGMENT

The author wishes to thank Messrs. M. Dawson and E. McBride for their efforts in building and testing the scale models used for this report. Project Directors P. E. Mayes and E. C. Hayden have contributed numerous suggestions and ideas to this work. .

It is a pleasure to acknowledge the support of the Navy Bureau of Ships under contract NOBSR 85243 and later under contract NOBSR 89229.

ABSTRACT

The feasibility of designing a wideband, high-efficiency vertical incidence antenna capable of providing either a single or split beam centered on the zenith has been investigated by the use of scale models. It was found that two log-periodic dipole array elements arranged in an H-plane array fed properly over ground would provide the required beam configuration in the H-plane.

A performance investigation as a function of the various design parameters was conducted where the design parameters' variation was limited to some extent by the practical considerations involved in an antenna designed for the 2 to 32 Mc frequency range. It was found that there existed a combination of parameters which would provide a reasonably good compromise between ideal pattern and impedance performance, the impedance performance being the more critical of the two.

During the parameter investigation some interesting antenna feed problems were encountered and investigated to the extent of solving the problems for the special applications involved in the model studies being conducted.

1. Introduction

This report describes the work that has thus far been done in an effort to design a practical, wideband, high efficiency, vertical incidence radio location array. As stated in Supplement #1 to the original proposal for contract Nobsr 85243,¹ there is a need for such an antenna to complement the oblique incidence steerable type D/F arrays at high angles of elevation and to furnish information on current ionospheric conditions so these conditions can be related to the D/F errors of the steerable type arrays.

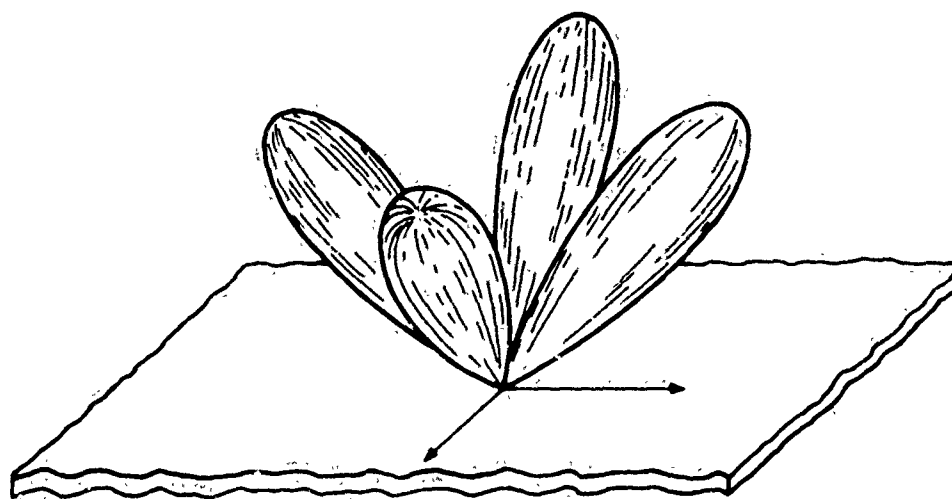
The general objectives in the design of the full-scale vertical incidence array as proposed are as follows: (1) the structure should be wide band in its operation, that is, the pattern and impedance characteristics of the structure should be essentially independent of frequency over the 2 to 32 Mc/s frequency range; (2) Since the array would be used for transmitting as well as receiving, it is necessary that the structure have good efficiency; (3) The structure should be capable of handling 30 KW peak power and an average power of at least 1 Kw; (4) The structure should be designed so that it is capable of withstanding the environmental conditions one would expect to find in the middlewestern United States.

The detailed design objectives are as follows: It is desirable for the array to consist of an arrangement of elements such that sum or difference modes of operation can be selected as desired in two orthogonal planes, (see Figure 1a and 1b). In the case of the sum mode, the single beam centered on the zenith should be approximately 90° wide between half power points. In the case of the difference mode the maxima of the four beams should be approximately 45° from the zenith, and the null between the four lobes should be at least 20 db down from the beam maximum. (See Figure 1c.)

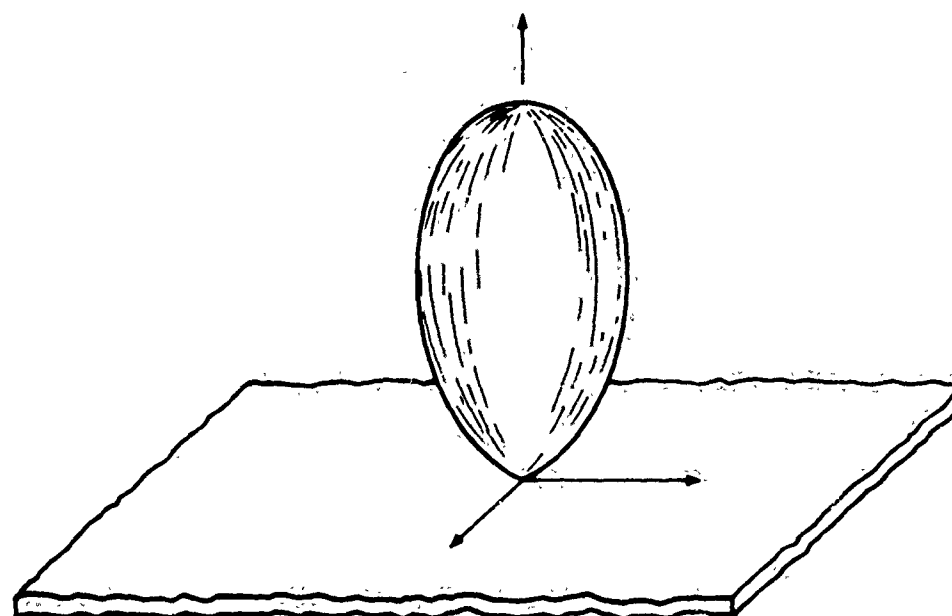
The impedance of the structure connected in either the sum or difference mode should be approximately 50 ohms with the input VSWR referred to 50 ohms less than 2:1 over the 2 to 32 Mc/s frequency range.

2. General Approach to the Design of the Vertical Incidence D/F Array

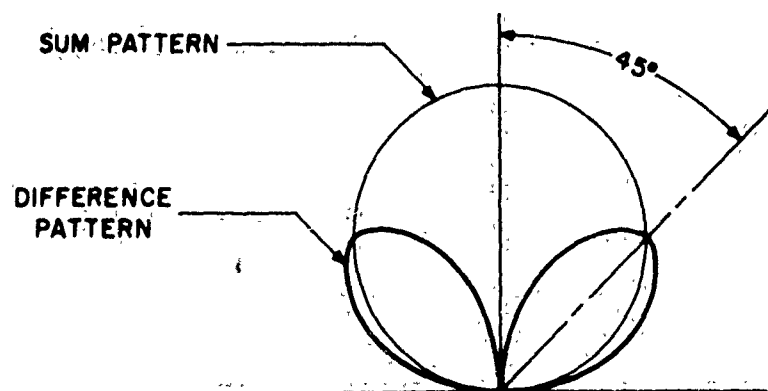
The first step in the design of the vertical incidence array was to select a structure which could be easily adapted as a basic element of the array. From a survey of the information available on log-periodic antennas,



(a) PICTORIAL VIEW OF THE RADIATION PATTERN OF A 4-ELEMENT ARRAY OPERATING IN THE DIFFERENCE MODE



(b) PICTORIAL VIEW OF THE RADIATION PATTERN OF A 4-ELEMENT ARRAY OPERATING IN THE SUM MODE



(c) DESIRED BEAMWIDTH OF THE SUM MODE AND BEAM LOCATION OF THE DIFFERENCE MODE

Figure 1.

the log-periodic dipole array shown in Figure 2 appeared to be the most promising for several reasons: (1) The log-periodic dipole array has well behaved single lobe, unidirectional, radiation characteristics as well as good impedance characteristics; (2) There is a great deal of practical design information available on this type structure;² (3) This type structure has been used for a similar application;³ (4) The general construction of this type structure is readily adaptable to low frequency applications.

Having selected the basic element of the array, the next problem was how to arrange the elements in an array to give the pattern performance desired. As was shown by DuHamel and Berry,⁴ it is possible to arrange basic log-periodic elements in a multi-element array. However, in order to realize frequency independent performance of such an array, it is necessary to arrange the elements so that the dimensions of the active region of the array remain constant in terms of wavelength. It is a known fact that the phase center of a log-periodic element is located approximately at a constant distance, d , in terms of wavelength from the vertex of the element, see Figure 3.⁵ In order to maintain a constant spacing, b , in terms of wavelength between the phase centers of adjacent elements in an array, it is necessary to locate the vertices of the elements of the array at a common point, V , with a constant angle, ψ , between the planes of the elements.

In the case of the proposed four-element vertical incidence antenna, it is necessary to array two cross sets of two elements each. Thus, placing four elements on the four faces of a pyramid and feeding elements located on opposite faces of the pyramid as an array is a compact and logical arrangement. See Figure 4.

To provide the desired pattern configuration symmetrically centered on the zenith, there is a choice of two possible arrangements of the pyramid with respect to the ground. If only high frequency operation were of interest, the array would be small enough to construct many wavelengths above the ground thus, the ground would have very little effect on the operation of the array. But, since the proposed full scale antenna is very large, it is impossible to get it high enough above the ground to achieve the so-called free space conditions. Thus, the logical arrangement of the array is one where the ground becomes part of the antenna. This is done by pointing the pyramid at the ground with the vertices of the dipole array elements meeting at a point just above the ground. This arrangement has the effect of including the image of the antenna as additional elements of the array in the proper manner to permit frequency-independent performance.

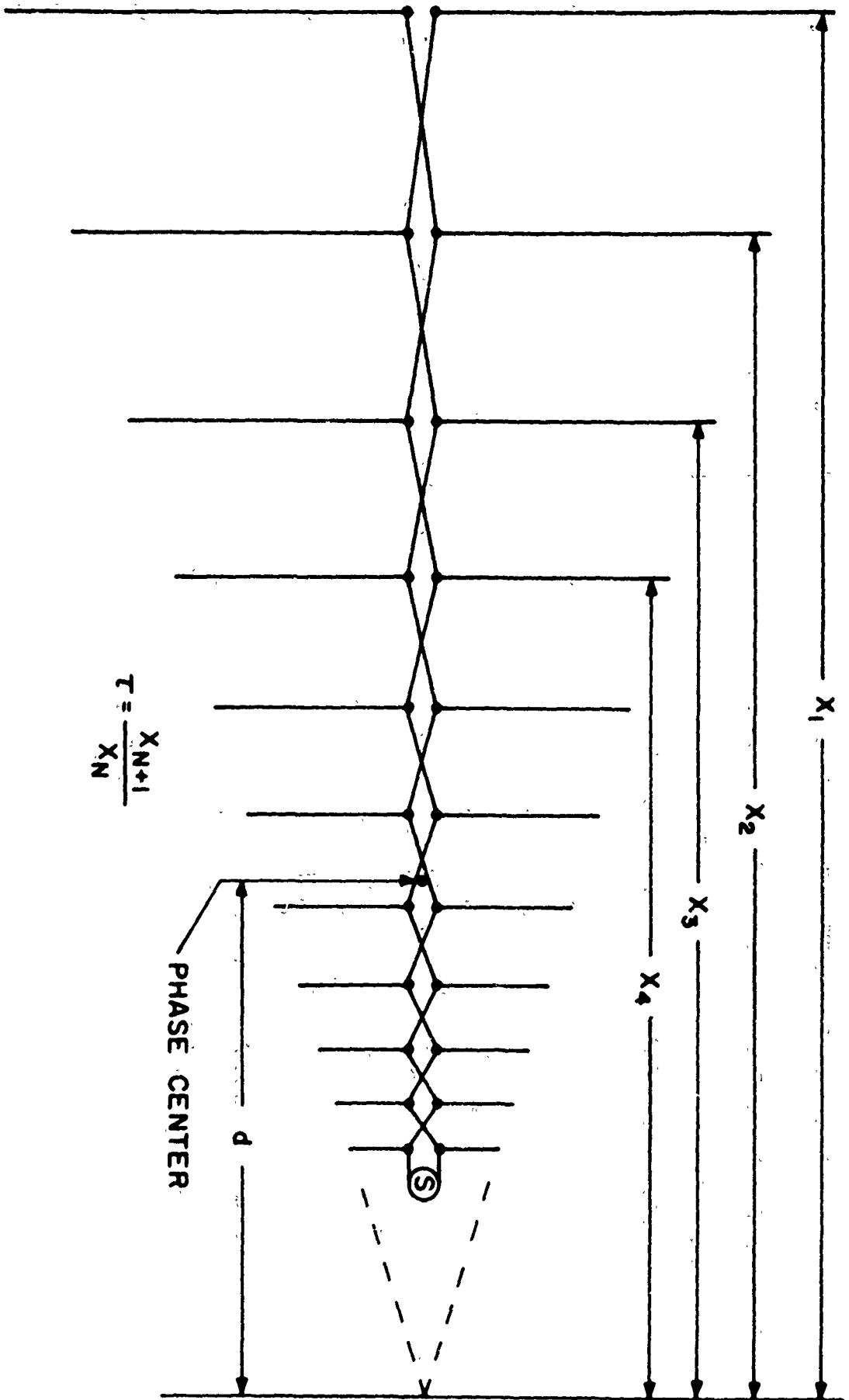
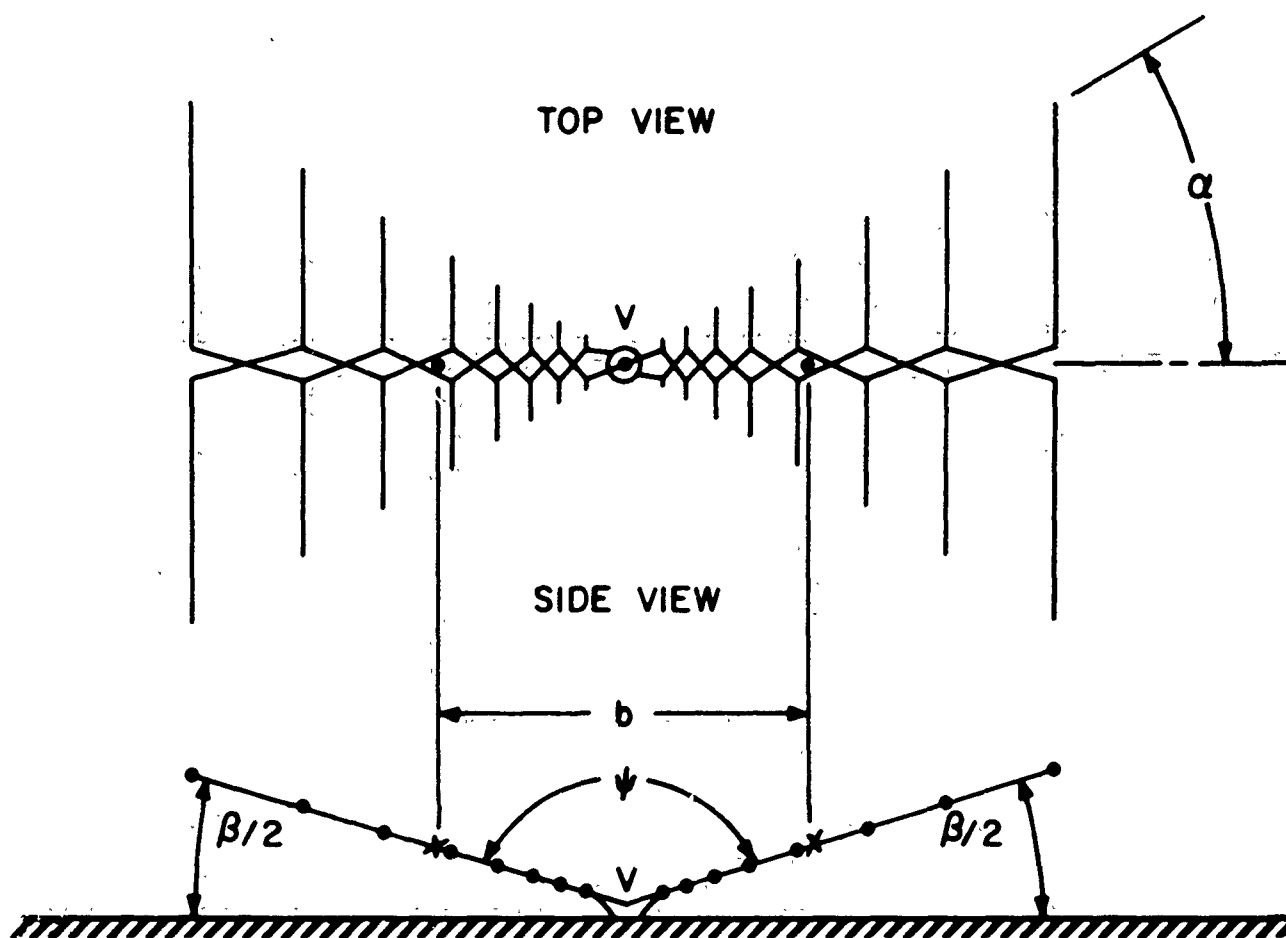


Figure 2. Log-periodic dipole array.



$$b = 2d \cos\left(\frac{180 - \psi}{2}\right) = \text{DISTANCE BETWEEN ELEMENT PHASE CENTERS}$$

Figure 3. Two element log-periodic dipole array over ground.

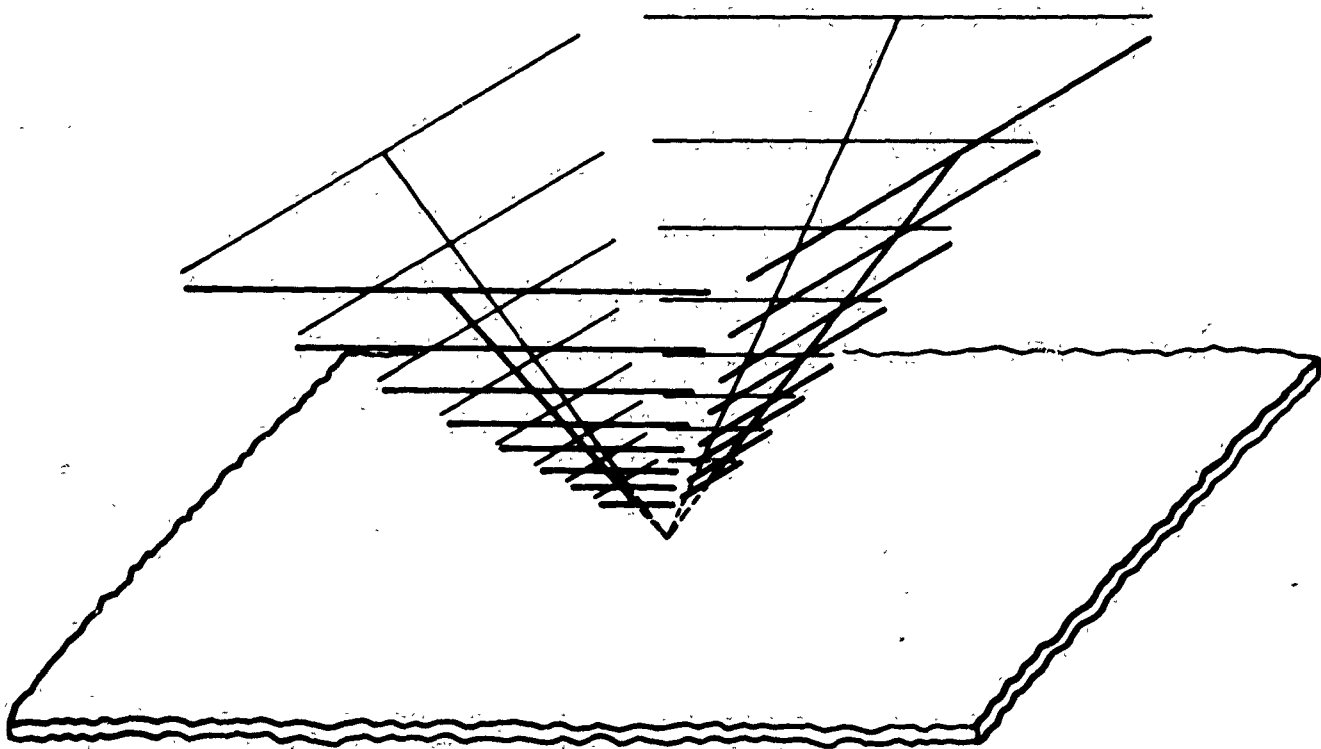


Figure 4. Four log-periodic dipole array elements forming the four sides of an inverted pyramid positioned over ground.

In the early part of the model pattern investigation, both arrangements were actually tried, and indeed, it was found that when the array was operated near the ground the one pointing at the ground gave the best performance.

Since this structure is ultimately being designed for the 2 to 32 Mc frequency range, some restriction as to the choice of the design parameters is imposed by physical size considerations. To better understand these problems, a short discussion of the physical sizes involved is in order (see Figures 5a and 5b). First of all, a wavelength at 2 Mc is 492 feet. This means that the longest dipole of a dipole array element will be approximately 250 feet in length. If the α angle of the dipole array is 22.5° , the length of the element from vertex to the longest dipole will be approximately 300 feet. If each element makes a 30° angle, $\beta/2$, with the ground the longest dipole will be 150 feet above the ground. In order to compensate for the sag that is inherent in such a structure, the tallest tower used to support the structure will be between 180 and 200 feet in height. The height of 200 feet for the supporting tower is just about a practical upper limit, thus the angle above ground is limited to approximately 30° . Actually the height of the towers depends on both the α angle and the $\beta/2$ angle the element makes with ground. If the α angle is increased the angle above ground can be increased to correspond to this practical upper limit of the tower height. Figure 5b shows the case where $\alpha = 30^\circ$ and $\beta/2 = 30^\circ$. In general, however, the smallest practical α angle is approximately 22.5° .

Since the T ratio determines the number of dipoles of each element with the number of dipoles largest for the largest T ratio, it is desirable to keep the T ratio as low as possible. The minimum number of dipoles is desirable from the standpoint of weight, ice loading, cost, etc. The above-mentioned limitations were kept in mind when designing the several models listed in Table (I).

3. Small Model Pattern Investigation

In order to gain insight into the effect of the various design parameters on the radiation characteristics of the two-element array pointed at the ground system, several pattern models, listed in Table I, were constructed and measured. These models were designed to have a low frequency limit of approxi-

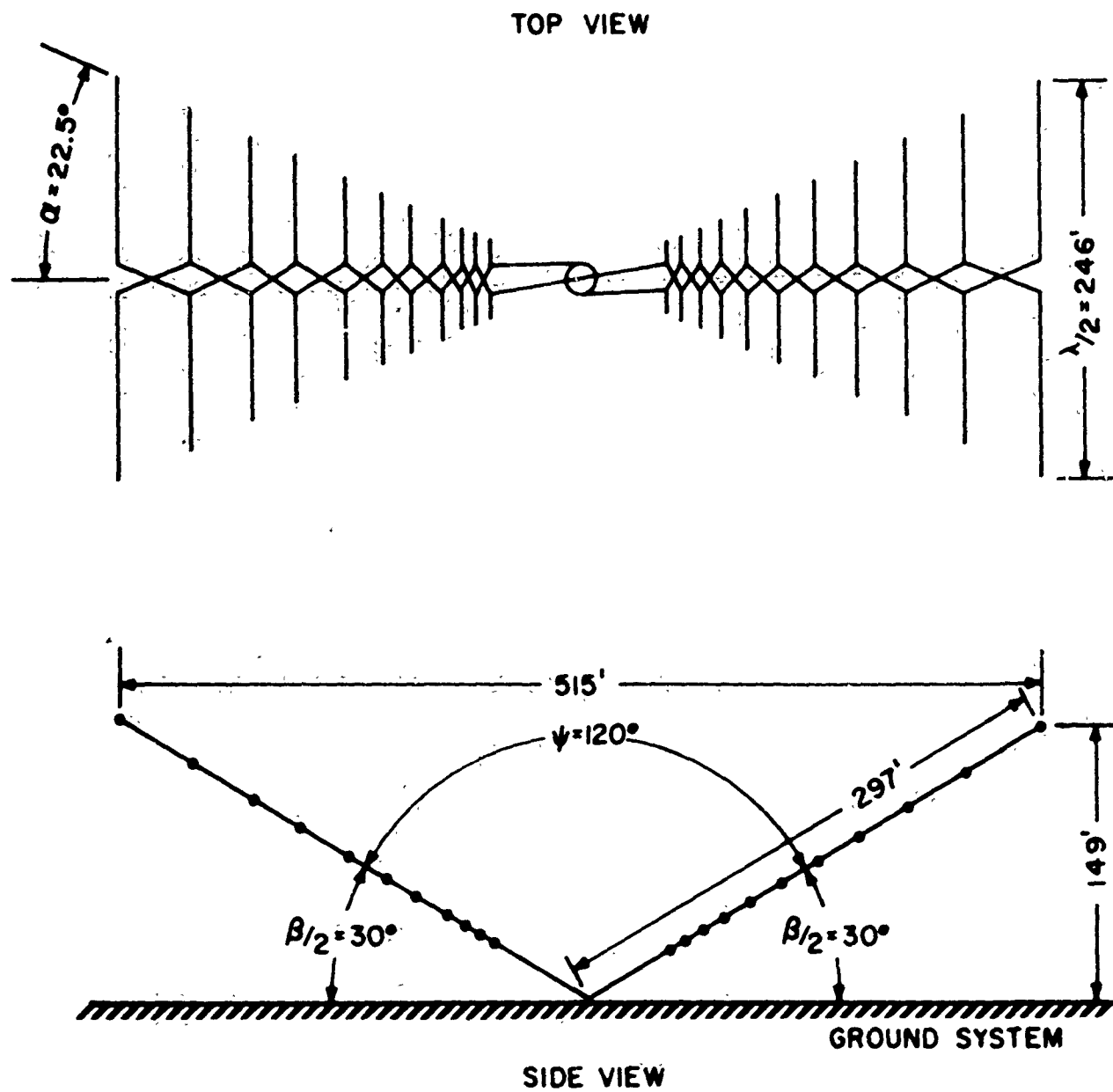


Figure 5a. Representative dimensions of a full scale 2-element vertical incidence array designed for the 2-32 Mc frequency range.

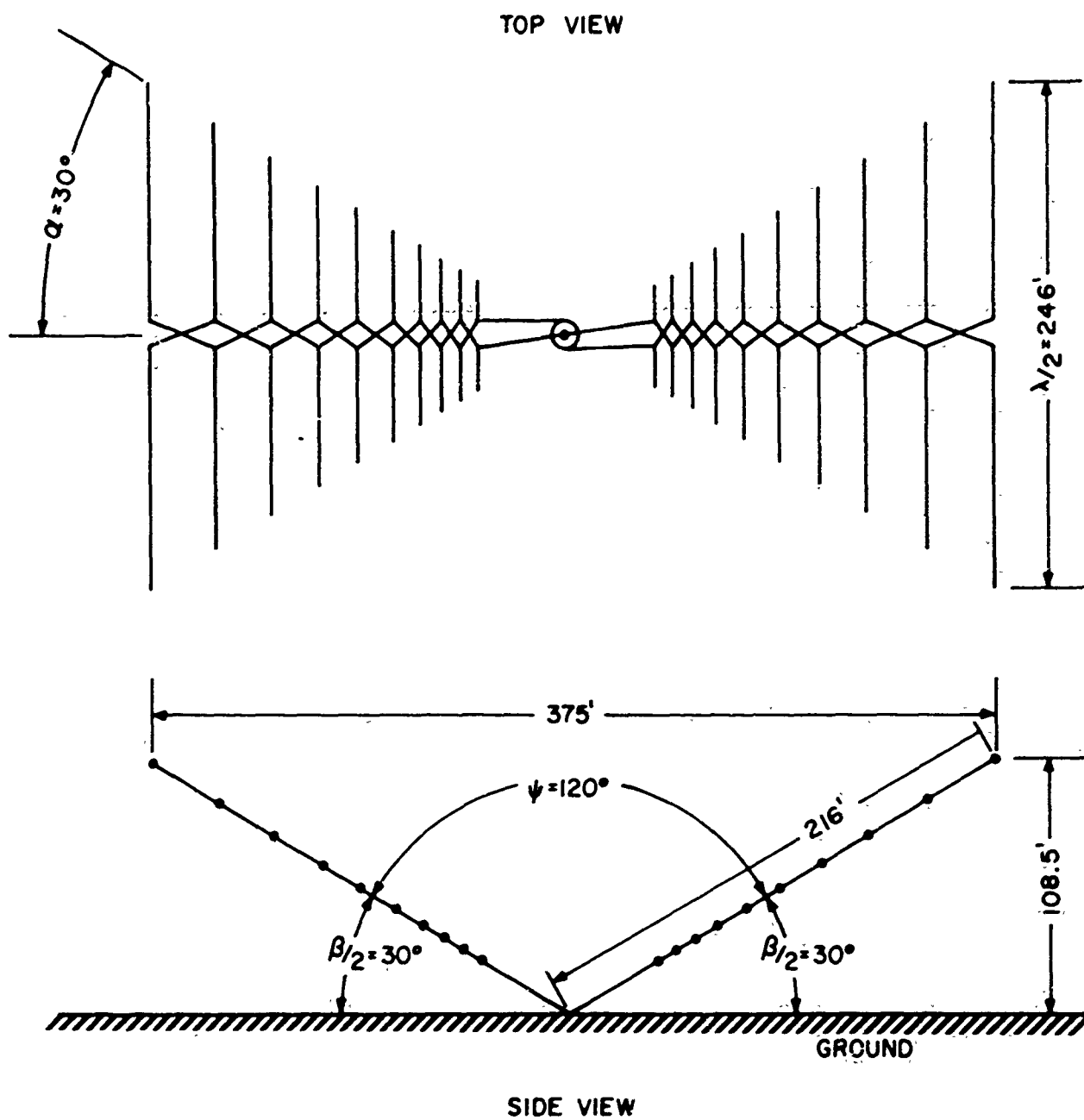


Figure 5b. Representative dimensions of a full scale 2 element vertical incidence array designed for the 2-32 Mc frequency range.

TABLE I

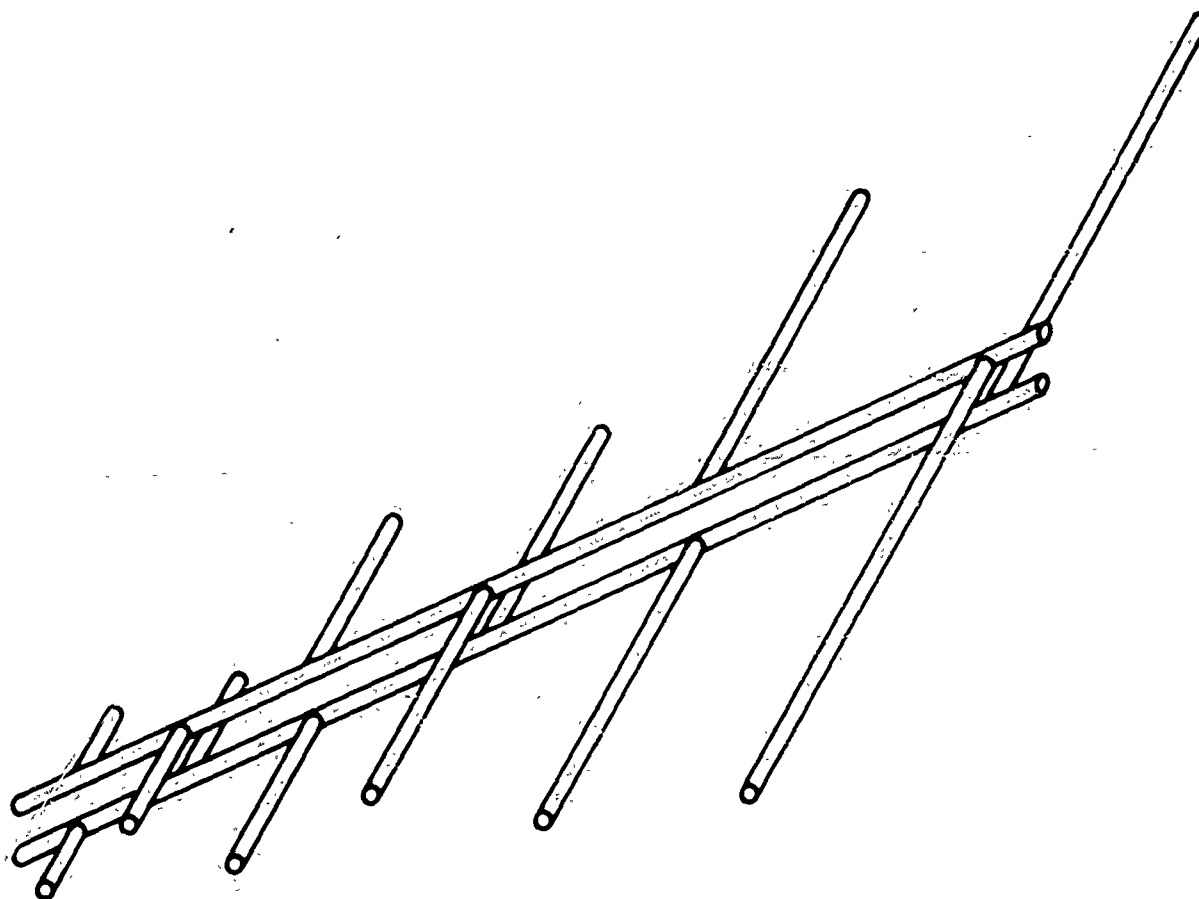
Antenna	α	τ	ψ	Lobes from zenith θ'
VI (AR) 2	30°	.84	90°	46°
VI (AR) 2B	30°	.84	120°	37.5°
VI (AR) 2C	30°	.84	150°	33.0°
VI (AR) 3A	37.5°	.84	130°	39.5°
VI (AR) 3B	37.5°	.84	150°	37.0°
VI (AR) 5	22.5°	.84	90°	45.3°
VI (AR) 5A	22.5°	.84	150°	28.0°
VI (AR) 6	37.5°	.707	150°	47.6°
VI (AR) 6C	37.5°	.707	130°	51.0°
VI (AR) 7	30°	.707	150°	38.5°
VI (AR) 7B	30°	.707	130°	42.5°
VI (AR) 8	30°	.775	150°	30.2°
VI (AR) 8B	30°	.775	120°	36.4°
VI (AR) 9	30°	.88	150°	34.35°
VI (AR) 10	22.5°	.707	150°	24°
VI (AR) 11	30°	.60	150°	22.8°
VI (AR) 11A	22.5°	.60	120°	28.4°
VI (AR) 12	22.5°	.50	150°	25.6°

mately 500 Mc were measured from 500 Mc to 2000 Mc in all cases and some were measured to 4000 Mc depending on the detail of construction of the dipoles near the feedpoint of the dipole array elements. In general, the models were constructed as shown in Figure 6a. The feed technique used for these models is shown in Figure 6b. More comments concerning the feed technique will be made later in the section on impedance measurements.

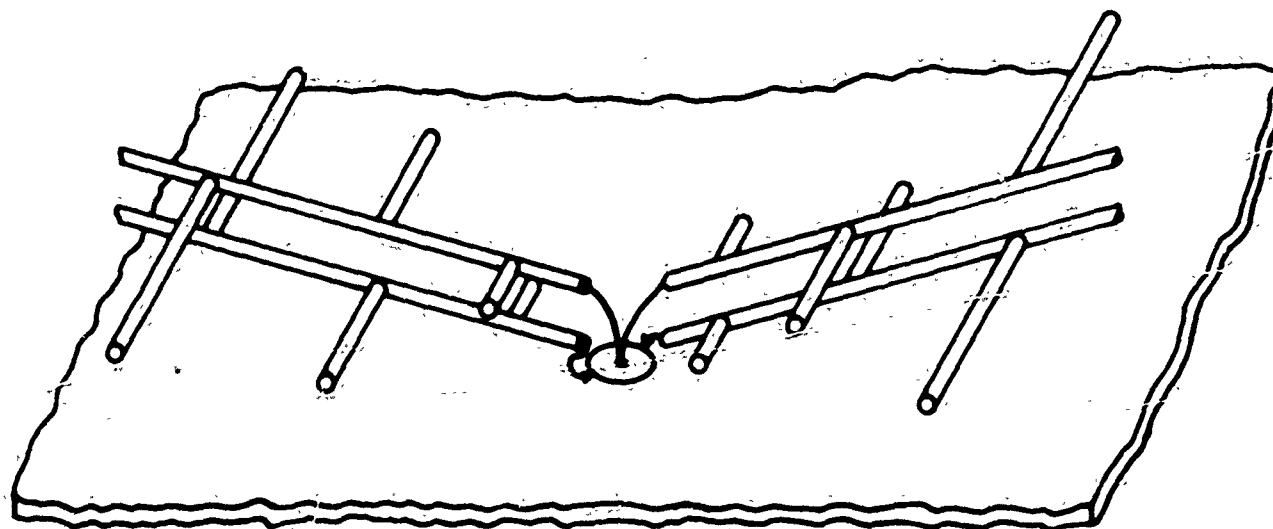
Typical sum and difference patterns of one of the models is shown in Figure 7. For this particular set of parameters ($\alpha = 30^\circ$, $\tau = .775$, and $\psi = 150^\circ$), the average angle from the zenith of the different lobes is 31° . The average null depth is approximately 25 db. The H-plane beamwidth of the sum mode is approximately 34° . The E-plane beamwidth is approximately the same as for a single dipole array element which is approximately 65° .

Figure 8 is a plot of the measured, average angles of the difference beams from the zenith as a function of the ψ angle for the various combinations of α and τ measured. Not enough models were tested to get detailed curves but the trends are clearly shown. Given a constant α angle, the beams are farther away from the zenith for the smaller ψ angle. This is exactly what one would expect, since by making the ψ angle smaller the aperture of the array becomes smaller and the pattern has a tendency to become broader. It is also shown, in general, that a given constant ψ angle the structures having the wider α angles have the greater beam spread. Here again the phase center of the structures with the wider α angle are nearer the apex of each element, thus the distance between the phase centers is smaller for the wider α angles and the effective aperture is smaller which results in a spreading of the beams. A phenomena for which there is at present no explanation is the variation of beam spread with τ ratio. From previous measured results on free-space models, it has been found that the variation of element phase center with τ is very slight. For the structures which have α angles of 30° and τ ratios of .707, .775 and .84, the one having a τ of .707 gave the widest beam spread for a given ψ angle.

Figure 9 is a plot of beam spread as a function of the α angle for several τ ratios and ψ angles. Actually this is the same data of Figure 8 presented as a function of α instead of ψ . The same trends as those of Figure 8 are apparent.



(a) GENERAL CONTRUCTION OF A SINGLE LOG-PERIODIC
DIPOLE ARRAY ELEMENT USED FOR PATTERN MEASUREMENTS



(b) TYPICAL FEED POINT OF A 2-ELEMENT ARRAY
PATTERN MODEL

Figure 6.

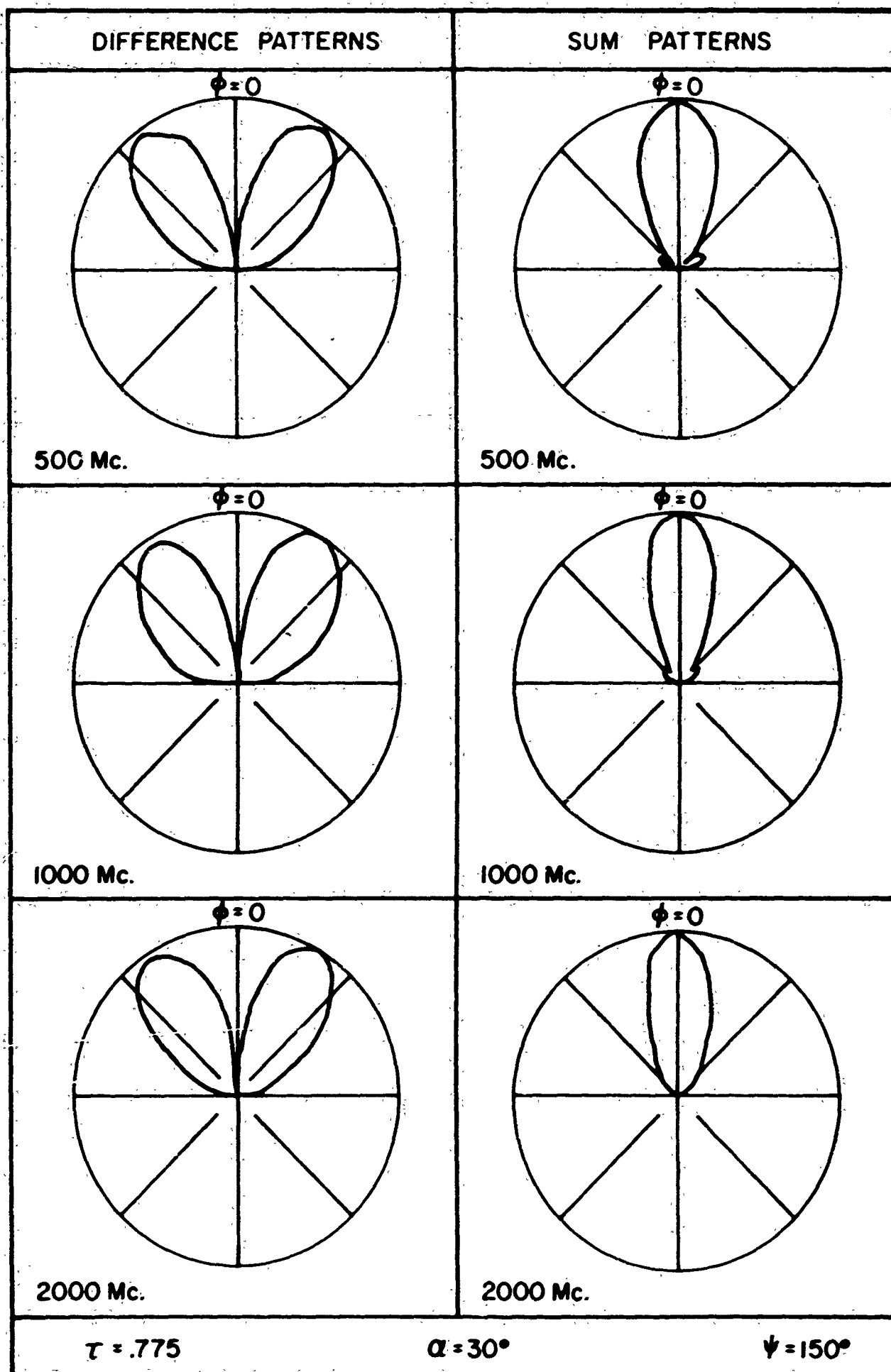
 $\psi = 150^\circ$

Figure 7. Representative sum and difference

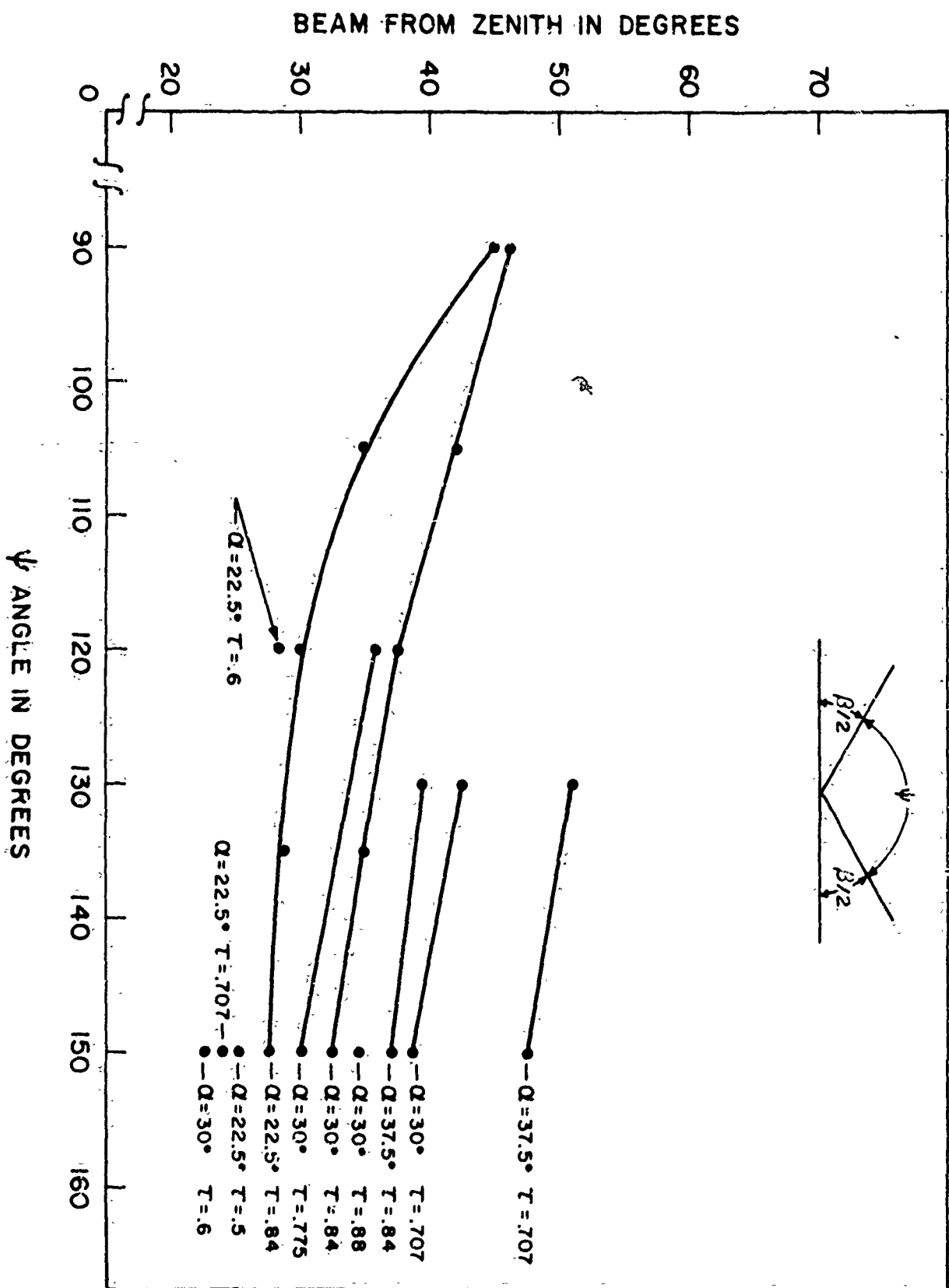


Figure 8. The measured angle from the zenith of the difference lobes as a function of ψ angle for several pattern models listed in Table I.

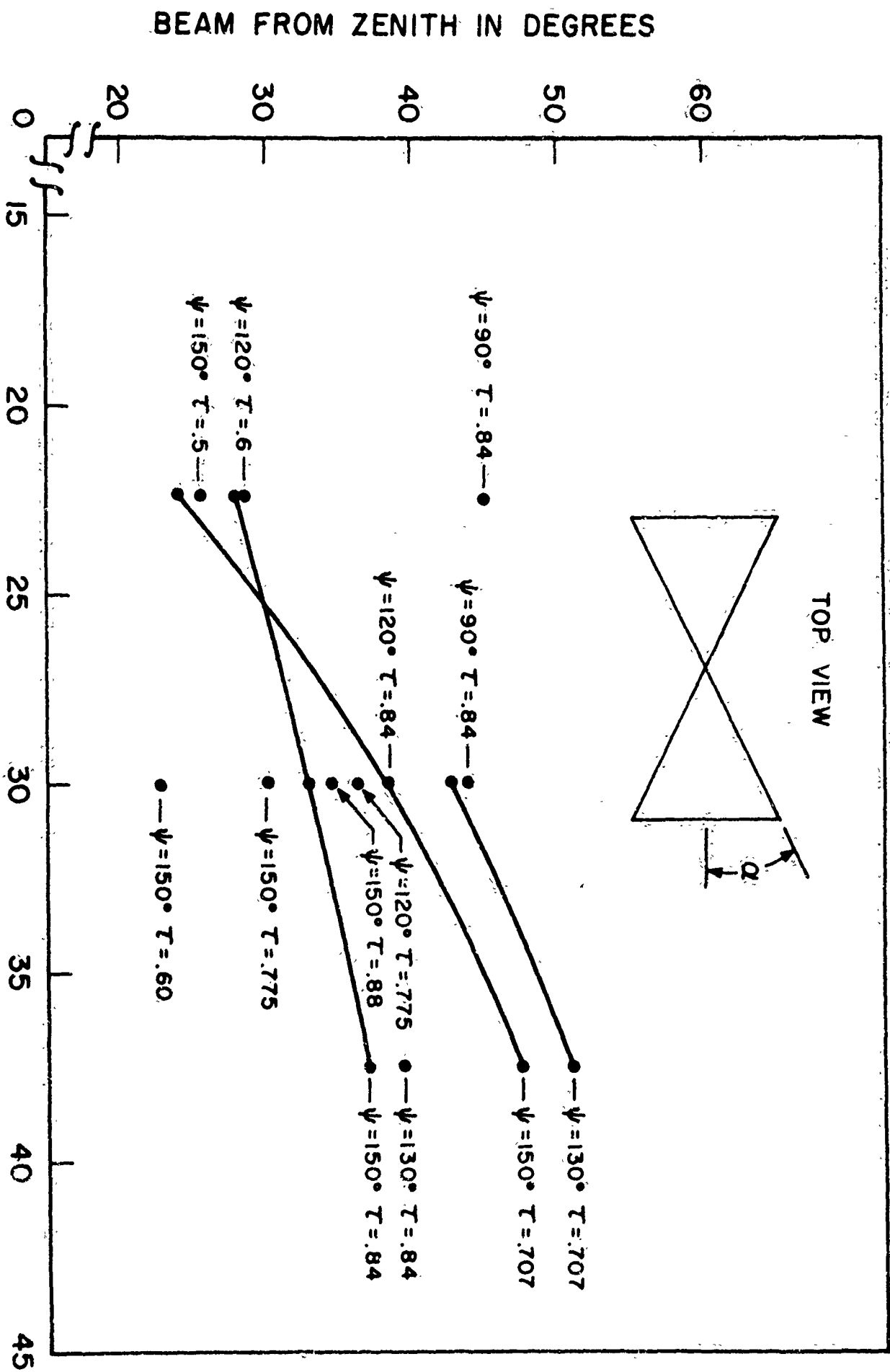


Figure 9. The measured angle from the zenith of the difference lobes as a function of α angle for several pattern models of Table I.

These curves in the last two figures represent the average performance of the models of Table I over the design parameters as indicated. However, occasionally a measured pattern would show mild to severe break-up as compared to the average performance for that model. This pattern break-up usually occurred near the high frequency limit of the particular model being considered. Also, the pattern break-up was usually accompanied by a sharp increase in the cross-polarization of the structure. The true reason for the pattern break-up was not known when the models were first tested. Several possible explanations for this difficulty were: (1) accuracy in the modeling techniques being inadequate; (2) incorrect feed technique; (3) the nearness of the ground system was effecting the current distribution on the structure in such a way that the performance of the structure was no longer frequency-independent, or (4) any combination of these possibilities.

Since all but a very few of the patterns over a wide frequency range for any one antenna were approximately the same, it was felt that basically the structure was functioning as a frequency independent antenna. Thus, although admittedly the ground was effecting the behavior of the structure, they were for all practical purposes frequency-independent. Since this pattern break-up occurred at the higher frequencies predominately, it suggested that perhaps the models should be constructed more accurately at the high frequency portion of the structure. In order to gain some insight into the effect of more accurate modeling, the structure shown in Figure 10 was constructed. As shown in the figure, the spacing between the feed line is uniformly tapered from the back of the structure to its vertex. This was accomplished by wrapping the feedlines around a conical dielectric rod. Also, the diameters of the dipoles are varied so that an approximate constant length to diameter ratio was maintained. The design parameters of this model are $\alpha = 22.5^\circ$ and $T = .84$. It was found that a single element of this type gave good free space patterns over a frequency range of 500 to above 7000 Mc., (Figure 11) which indicated that the better modeling techniques used had substantially improved the performance of this basic element. Two identical elements arranged in an array with a ψ angle of 150° produced the sum and difference patterns shown in Figure 12. For the most part, these patterns were quite

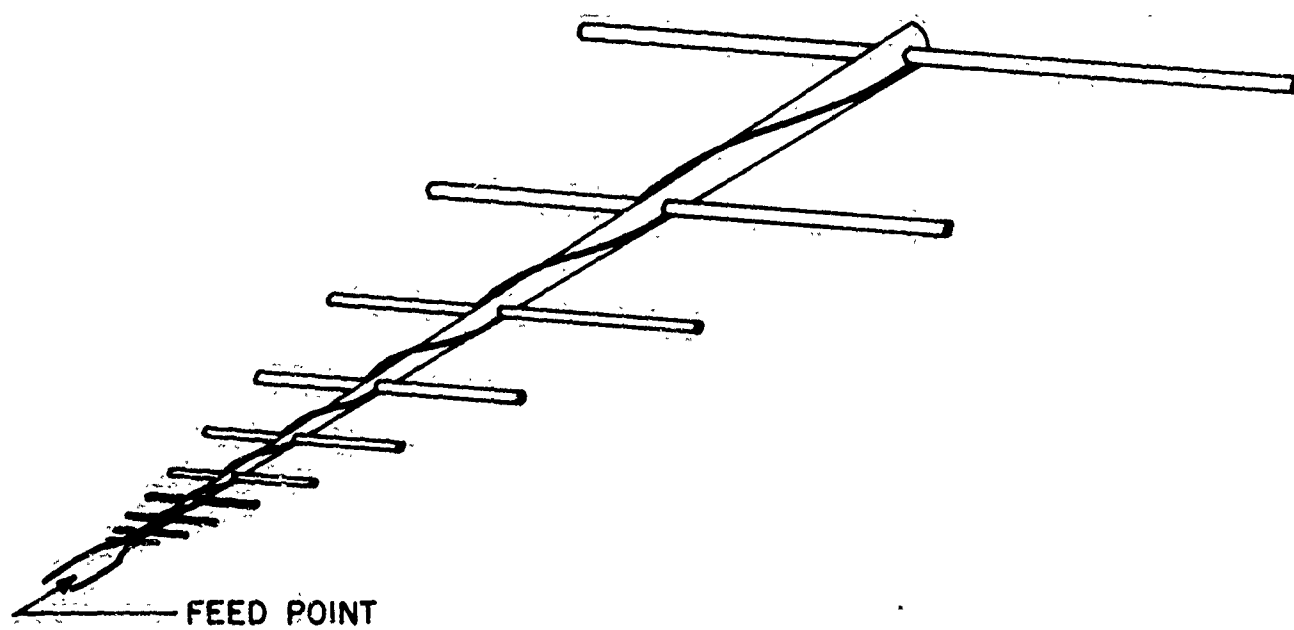


Figure 10. High frequency log-periodic dipole-array element model.

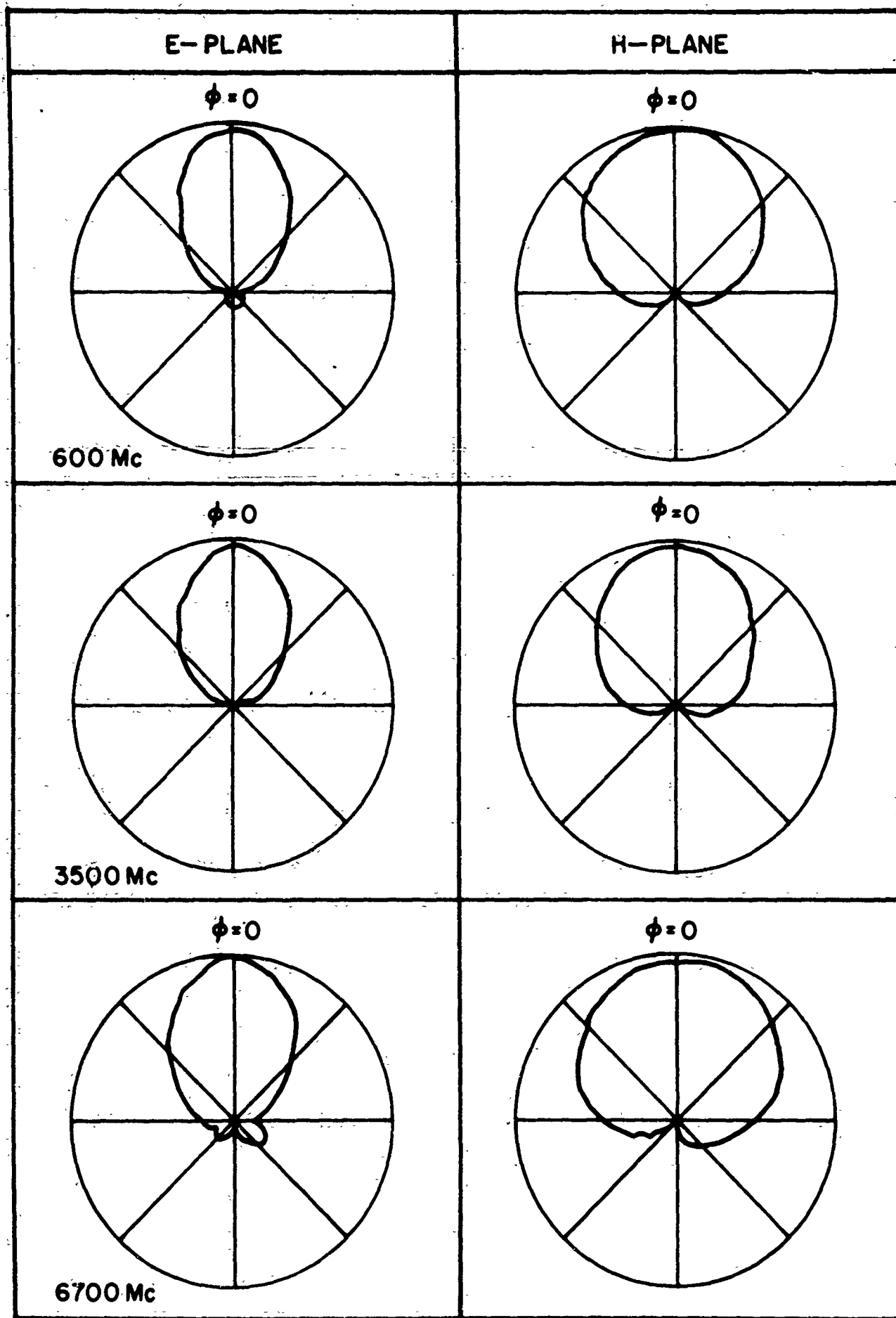


Figure 11. Representative free space patterns of the single element high frequency dipole array model.

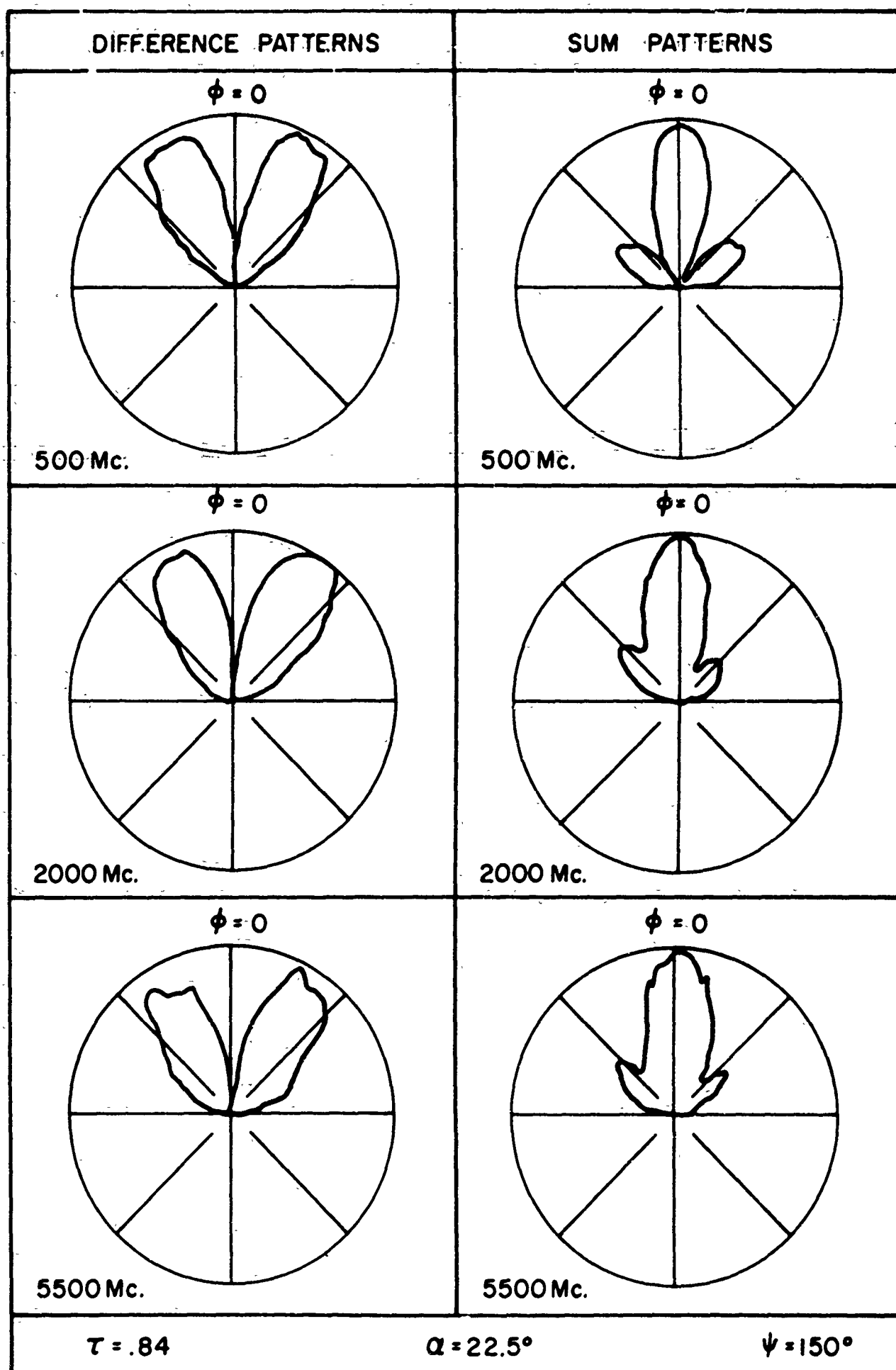


Figure 12. Representative sum and difference patterns of the high frequency model of a two element vertical incidence array.

good over the frequency range of 500 to 5500 Mc. There were a few frequencies where an unbalance of difference lobes was observed; however, this unbalance probably was due to the two elements not being exactly identical.

The maxima of the difference lobes remained at an average angle of 28° from the zenith. The sum patterns, taken over the same frequency range, gave an average half power beamwidth of 28° .

In general, this model showed that a structure of this type could be constructed to function over a wide frequency range without appreciable pattern break-up.

4. Pattern Calculations

To methodically investigate the effects of design parameter variation on the performance of an antenna experimentally, requires that a model be constructed and measured for each value of the parameter under investigation while holding all other parameters constant. If the number of parameters is large and if the range of each parameter is relatively wide, then the number of models required is extremely large and a great deal of time is required to construct and measure the models. However, if one is able to devise an ideal model which closely approximates the performance of the actual antenna and if a mathematical formulation can be derived which represents the performance of the ideal model as a function of the various design parameters, then a high-speed computer can be used to calculate the performance of the ideal model over the range of each design parameter in a very short time.

The only way to optimize the design of any antenna is to investigate methodically its performance as a function of the design parameters over an adequate range of these parameters.

In the preceding section, the experimentally obtained performance of the vertical incidence antenna was given for a few models. But not enough data were obtained to plot complete curves of antenna radiation performance as a function of major design parameters α , τ , and ψ . In order to select the combination of these parameters which give the optimum radiation performance (within limits imposed by a full scale model consideration), a great deal more data would be necessary.

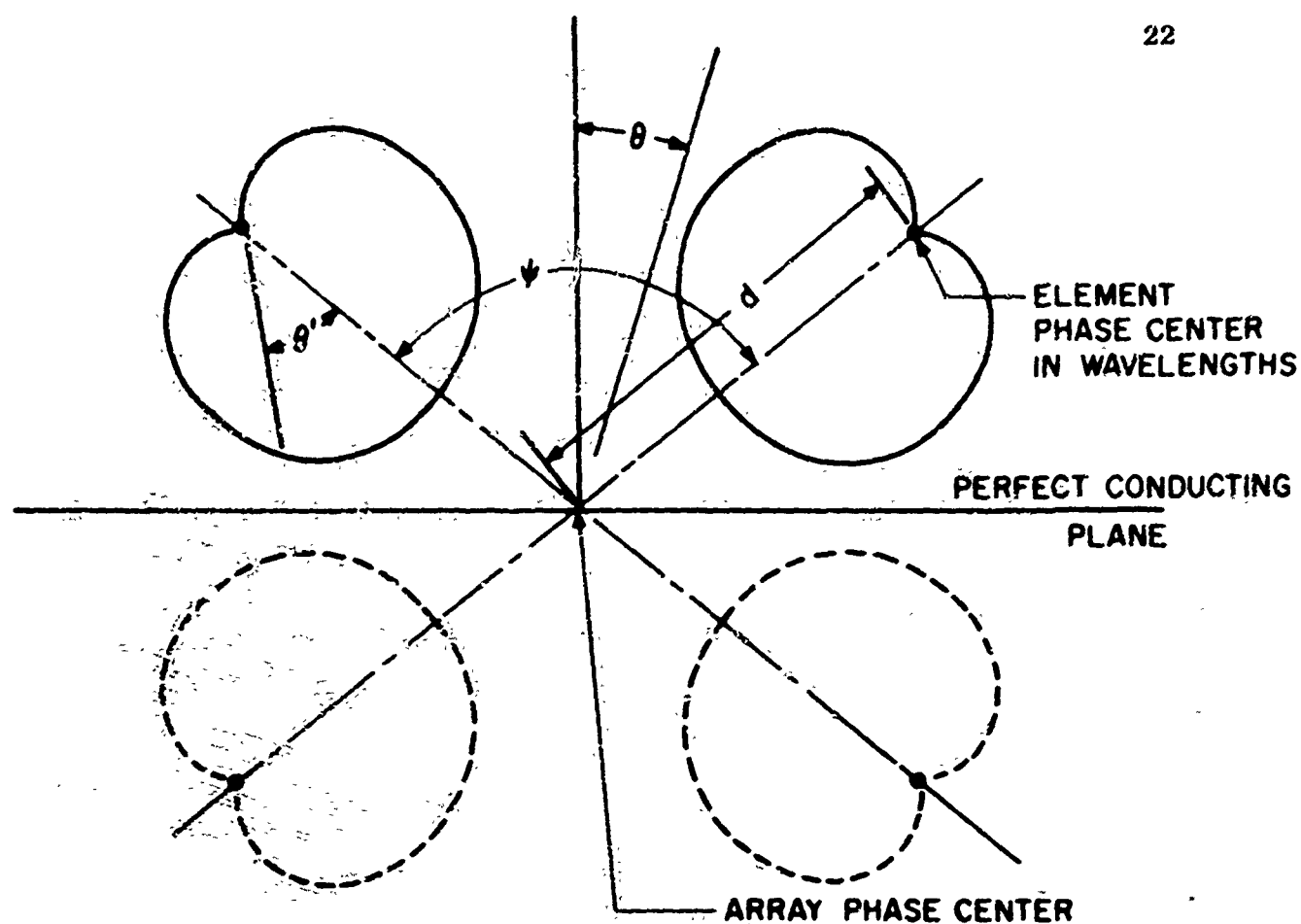
Observing this fact prompted an attempt to calculate the radiation patterns of the antenna as a function of the design parameters. The formulation of the problem was as follows: If one assumes that the ground system is a

perfect conductor, then Figure 13a shows the antenna and its image. This assumption is justified since in practice an artificial ground system would be provided for the antenna. When the image is included, the effect is that of having a four-element array instead of the apparent two-element array. Now, by choosing the mode of operation (sum or difference), one establishes the phase relation of the currents in the elements of the array. In the case of the difference mode, for example, the currents in the two real elements are 180° out of phase. It then follows from the theory of images that the currents in the images are 180° out of phase and that currents of an element are 180° out of phase with its image.

The calculation of the pattern for the array and its image would be very simple if the radiation characteristics of the elements were omnidirectional. However, as shown in the figure, the element patterns are unidirectional. To simplify this problem, a function $E(\theta') = \cos^M \frac{\theta'}{2}$ was assumed to represent the radiation pattern of each element. The exponent M was chosen so that the beamwidth of the assumed pattern was equal to the average measured beamwidth of the element being represented; the angle θ' is the angle from beam maximum of the element.

Using this assumed element pattern, the formula shown in Figure 13b was derived. The d in the formula is as was defined in section 2—the distance in wavelengths between the vertex and phase center of each element. The phase center of the array was assumed to be at the point where the vertices of the elements and their images meet. The parameter ψ appears in the formula. However, the parameter α is accounted for by the value of d/λ . Figure 14 shows a plot of d/λ as a function of α angle taken from a paper by Carrel². The parameter τ is accounted for in the choice of M in the formula for the element radiation pattern.

Using the formula, sum and difference patterns for the two-element vertical incidence array were calculated for values of ψ from 90° to 160° . For this case, $d/\lambda = .35$, corresponded to an α angle of approximately 30° and an element H-plane beamwidth of 130° was assumed. This assumed beamwidth corresponds approximately to an element having a τ ratio .84 and an α angle of 30° . These patterns are shown in Figures 15 and 16.



(a)

ELEMENT PATTERN:

$$E(\theta') = \cos^M \frac{\theta'}{2}$$

ARRAY PATTERN:

$$|E(\theta)| = \left| \cos^M \frac{1}{2} (180 - \frac{\psi}{2} - \theta) e^{-j[\beta d \cos(\frac{\psi}{2} + \theta) + \frac{\pi}{2}]} \right. \\
+ \left| \cos^M \frac{1}{2} (\frac{\psi}{2} - \theta) e^{-j[-\beta d \cos(\frac{\psi}{2} - \theta) - \frac{\pi}{2}]} \right| \\
+ \left| \cos^M \frac{1}{2} (180 - \frac{\psi}{2} + \theta) e^{-j[\beta d \cos(\frac{\psi}{2} - \theta) - \alpha]} \right| \\
\left. + \left| \cos^M \frac{1}{2} (\frac{\psi}{2} + \theta) e^{-j[\beta d \cos(\frac{\psi}{2} + \theta) + \alpha]} \right| \right|$$

FOR SUM MODE

$$\alpha = -\frac{\pi}{2}$$

FOR DIFFERENCE MODE

$$\alpha = \frac{\pi}{2}$$

(b)

Figure 13. Diagram of a 2-element vertical incidence array over perfect ground and formula used to calculate sum or difference patterns for this array.

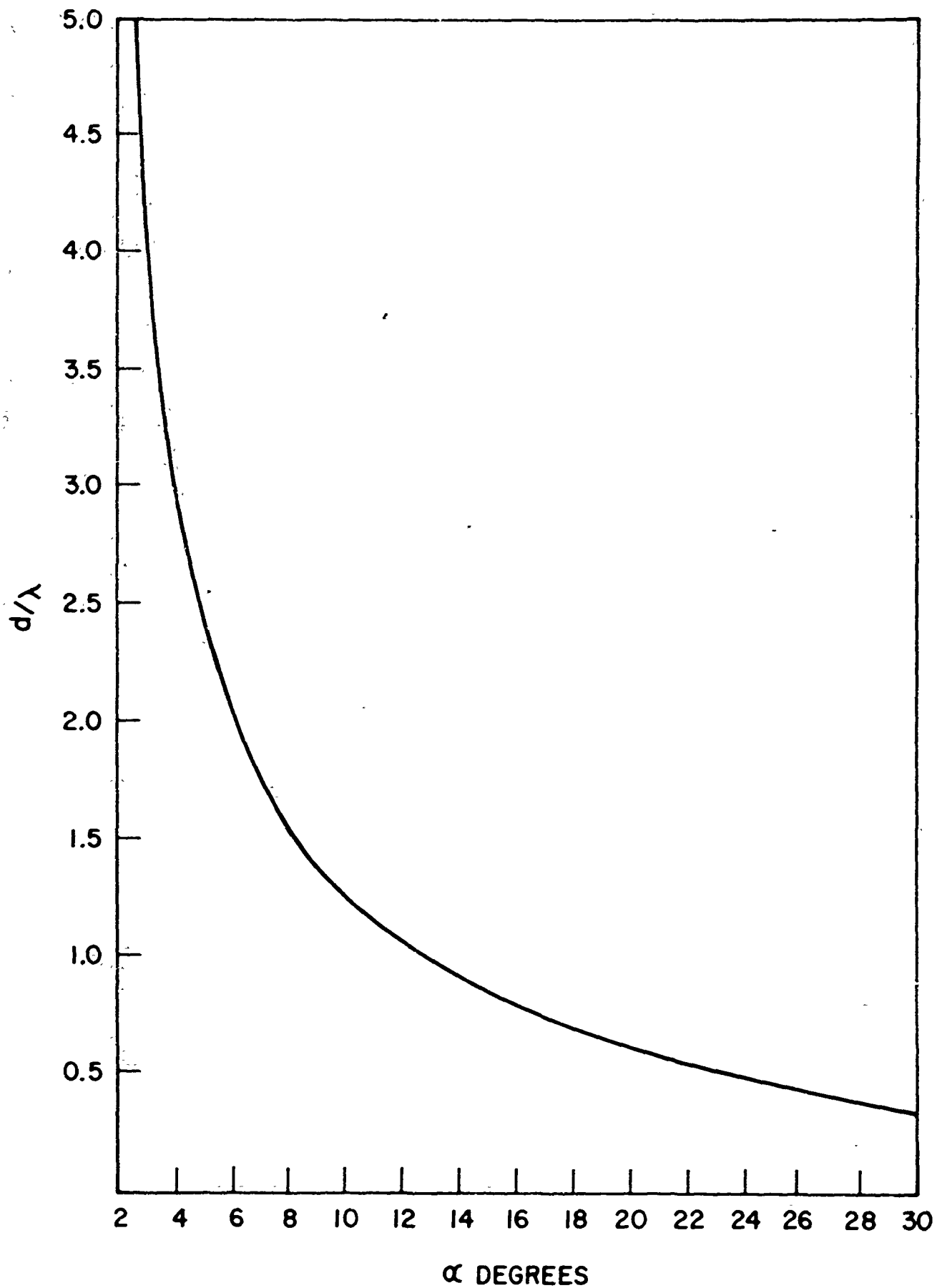


Figure 14. Location of phase center from the vertex of a log-periodic dipole array in terms of wavelength as a function of α angle.

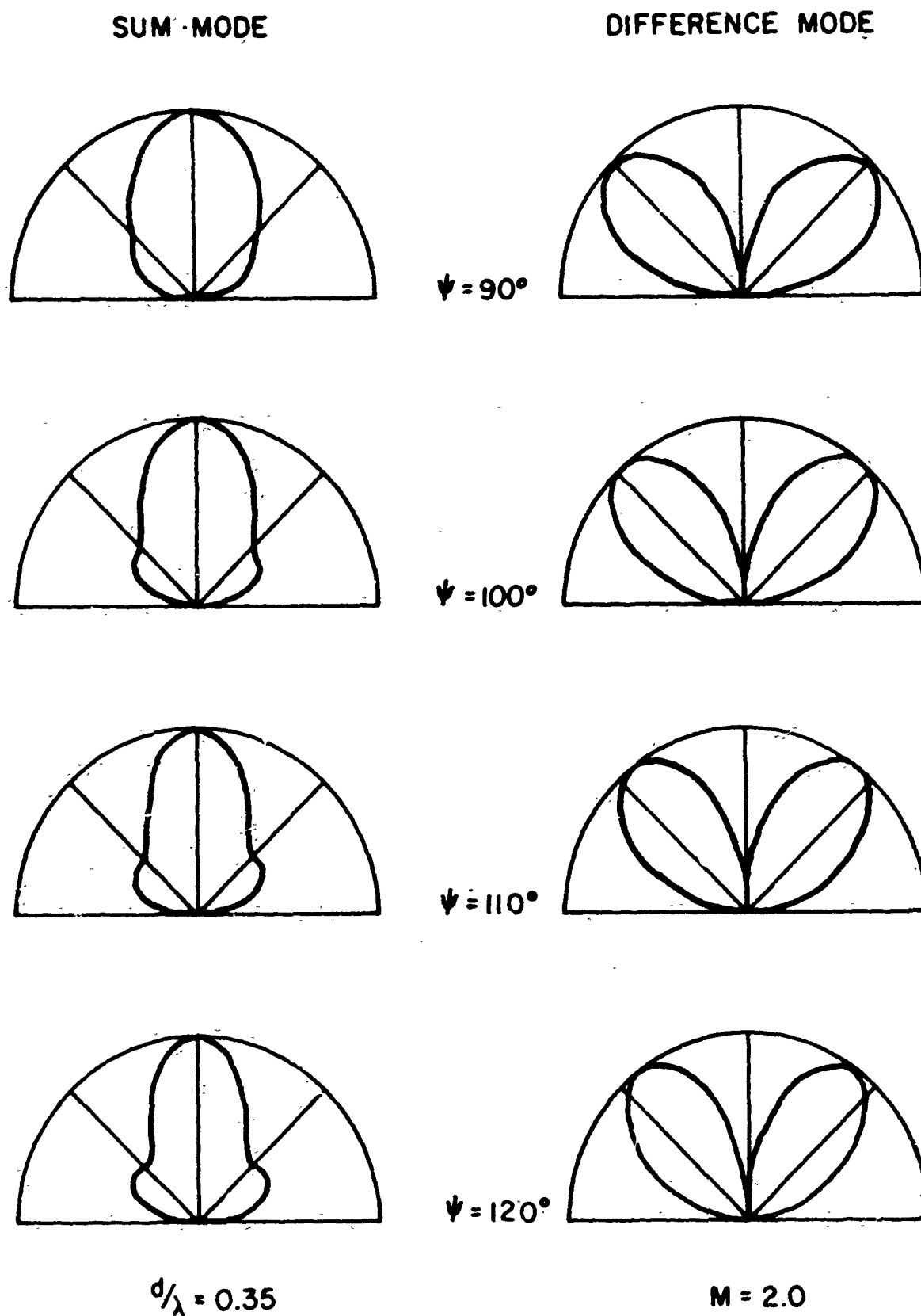


Figure 15. Calculated sum and difference patterns of the two element log-periodic vertical incidence array.

SUM MODE

DIFFERENCE MODE

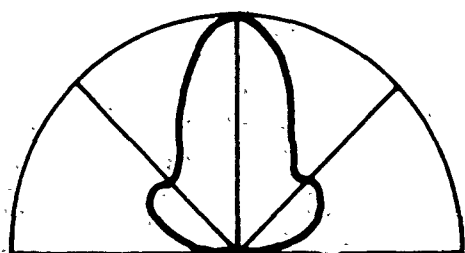
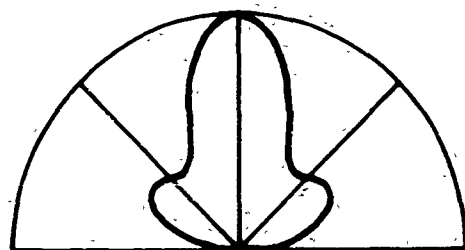
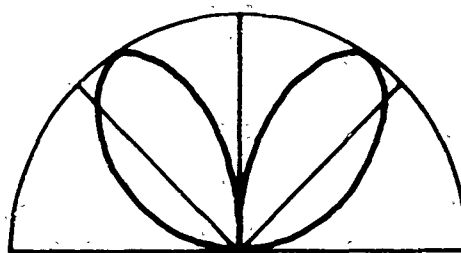
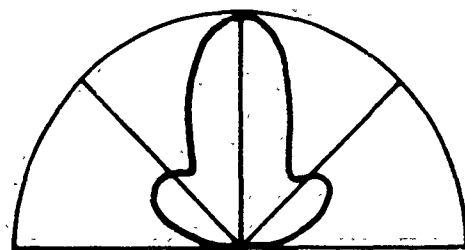
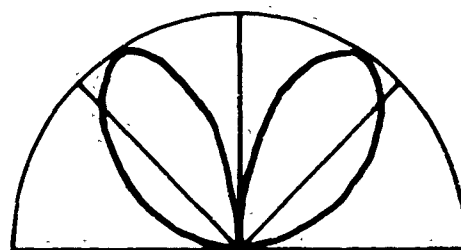
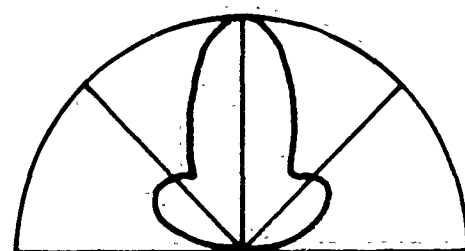
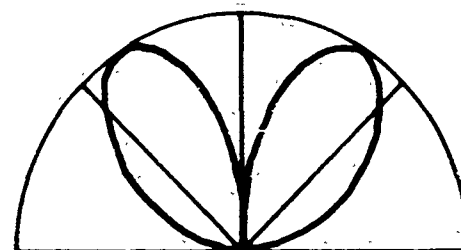
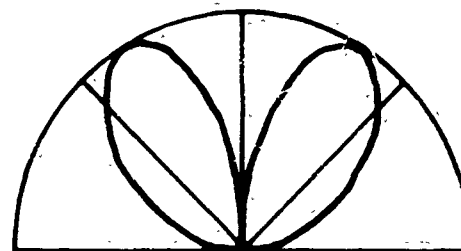
 $\psi = 130^\circ$  $\psi = 140^\circ$  $\psi = 150^\circ$  $\psi = 160^\circ$  $d/\lambda = 0.35$ $M = 2.0$

Figure 16. Calculated sum and difference patterns of the two element log-periodic vertical incidence array.

Figure 17 is a comparison of calculated difference beam locations with the available corresponding measured values read from the graph of Figure 8. The agreement as to difference beam location is reasonably good.

Another set of parameters were chosen and again the sum and difference patterns were calculated as a function of ψ angle, (see Figures 18 and 19). In this case, corresponding to an α angle of 22.5° , a $\frac{d}{\lambda} = .53$ was chosen. The beamwidth of the element was chosen to be approximately 110° . This corresponds approximately to a log-periodic dipole array having an α angle of 22.5° and a T ratio of .84.

Here again, the difference patterns were relatively well-behaved and compare reasonably well with the measured values (see Figure 20). The sum mode patterns show excessive sidelobes as compared to the measured patterns (see the case of $\psi = 150$ in Figure 12, for example). Apparently, the close proximity to ground changed the current distribution of the elements of the measured model in such a way as to reduce the overall sidelobe level. Or, in effect, the phase center location of the measured elements is not the assumed free-space phase center location used in the calculations.

Figure 21 is a comparison of the calculated and measured sum mode beamwidths as a function of ψ angle for the two cases calculated. For the case where $\alpha = 22.5^\circ$, reasonably good agreement between calculated and measured patterns occurred at $\psi = 90^\circ$, 105° , and 150° . But, for the other measured values, the agreement was not very good. In general, for both cases the measured patterns had a wider beamwidth than the calculated ones. The reason appeared to be due to the fact that the calculated patterns had definite sidelobes, whereas most of the measured patterns showed signs of sidelobes appearing but did not actually have large sidelobes. This is another indication of an incorrect assumed element phase center location.

Additional pattern calculations were contemplated, but due to the contract being revised, work was suspended at this point.

5. Impedance Measurements

A brief search was made in the available literature to determine how much information was available, if any, on the impedance of the type of structure being considered here. It was known that commercial firms had

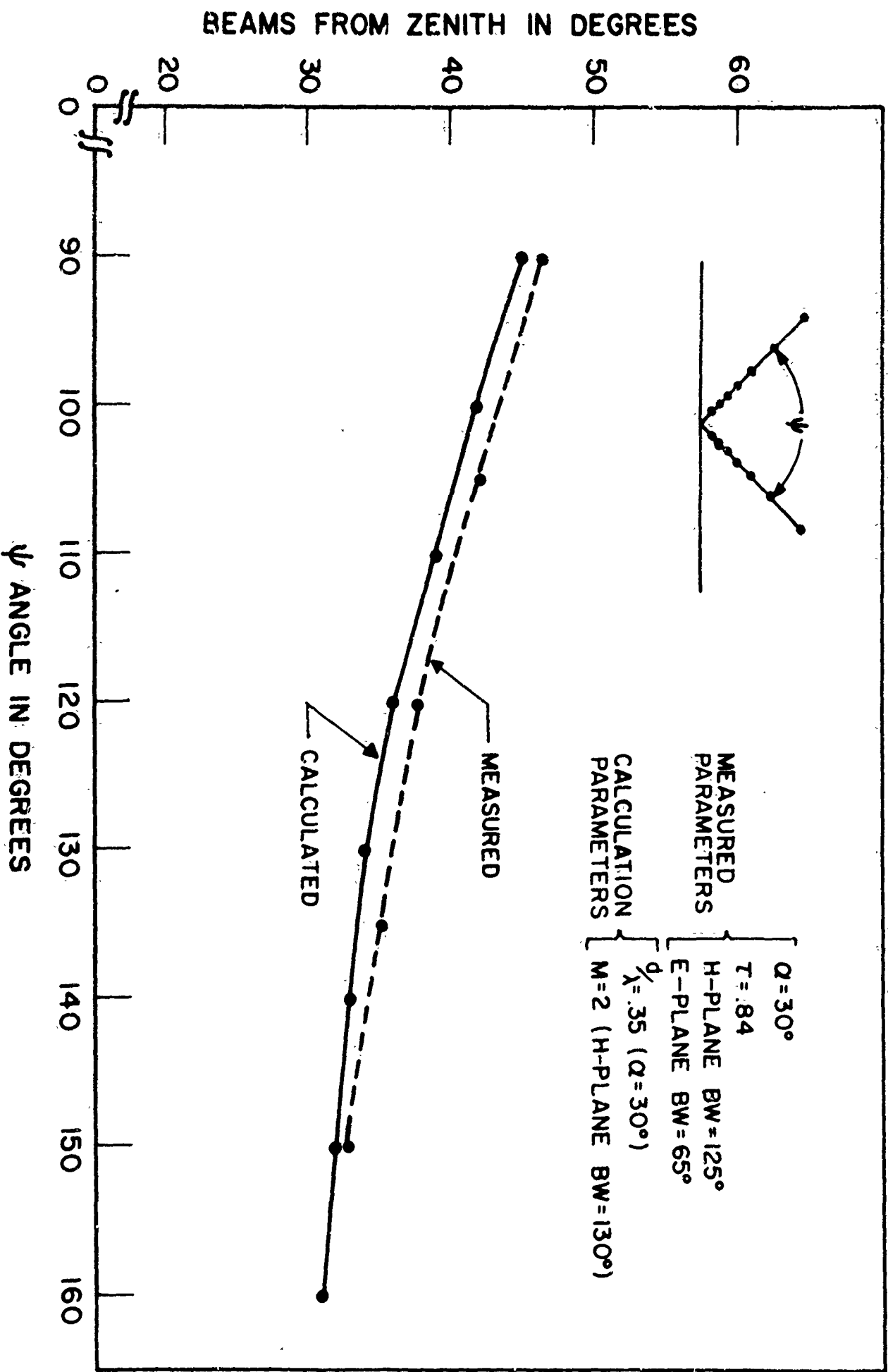


Figure 17. Measured and calculated difference mode beam location from the zenith as a function of ψ angle.

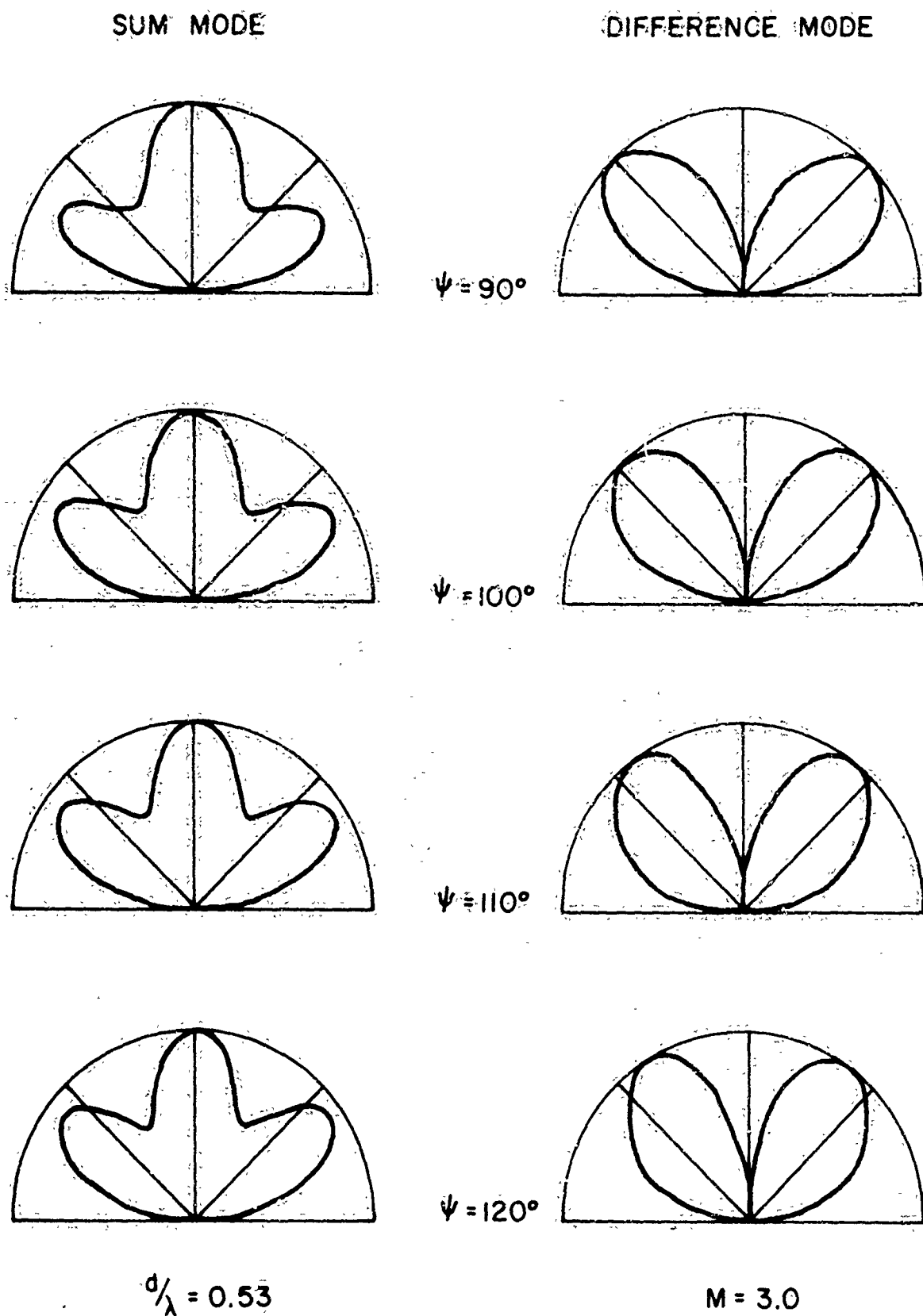


Figure 18. Calculated sum and difference patterns of the two element log-periodic vertical incidence array.

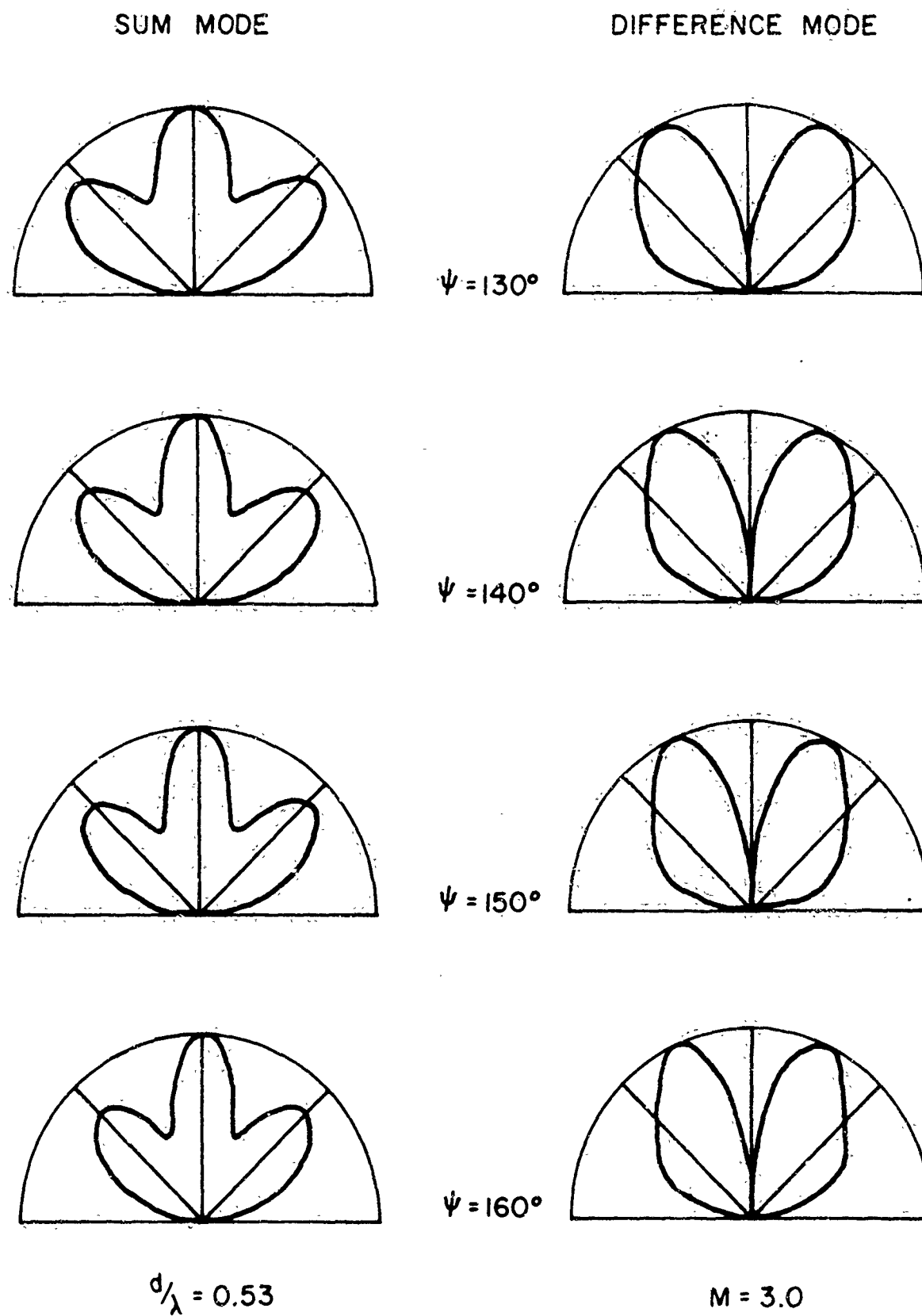


Figure 19. Calculated sum and difference patterns of the two element log-periodic vertical incidence array.

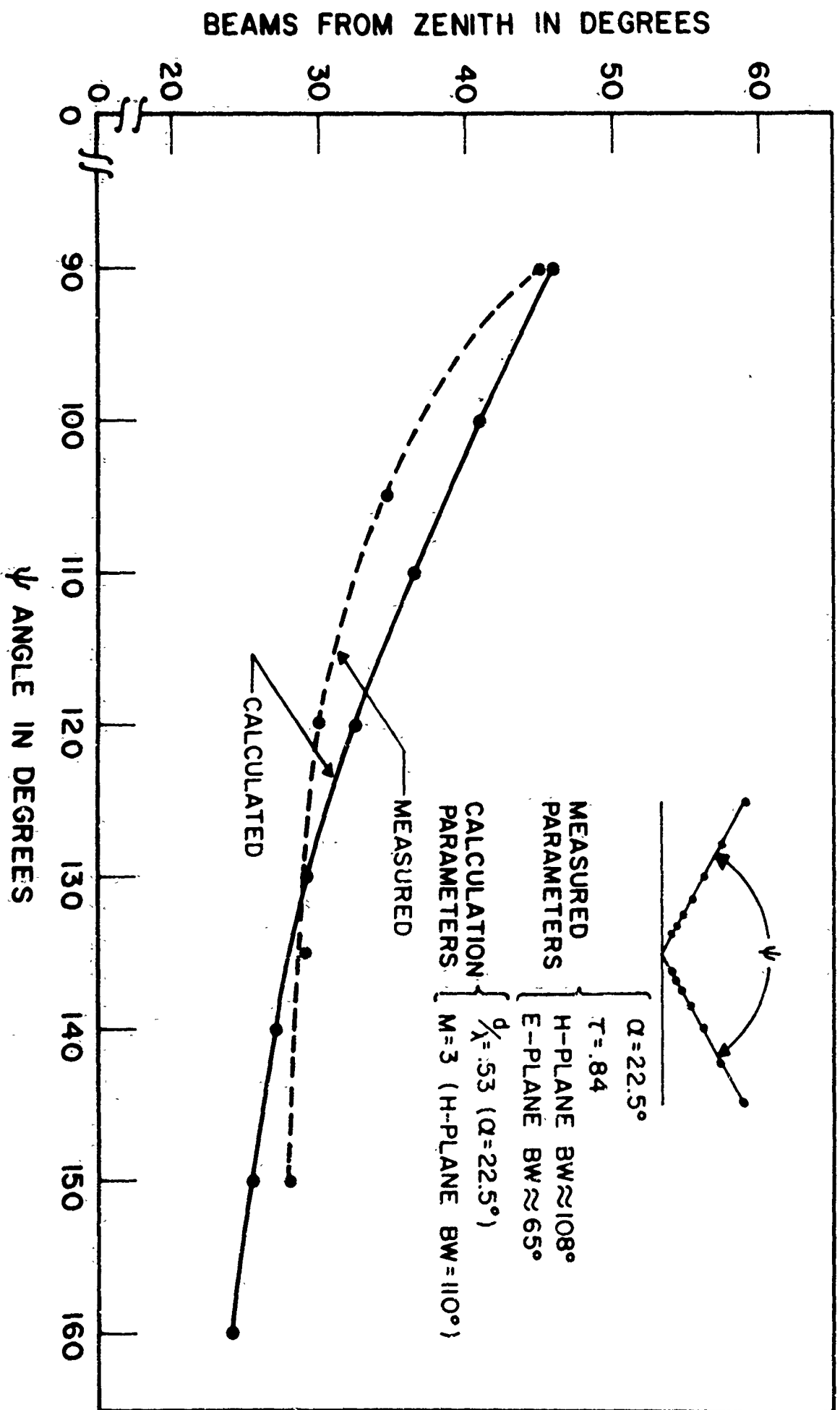


Figure 20. Measured and calculated difference mode beam location from the zenith as a function of ψ angle.

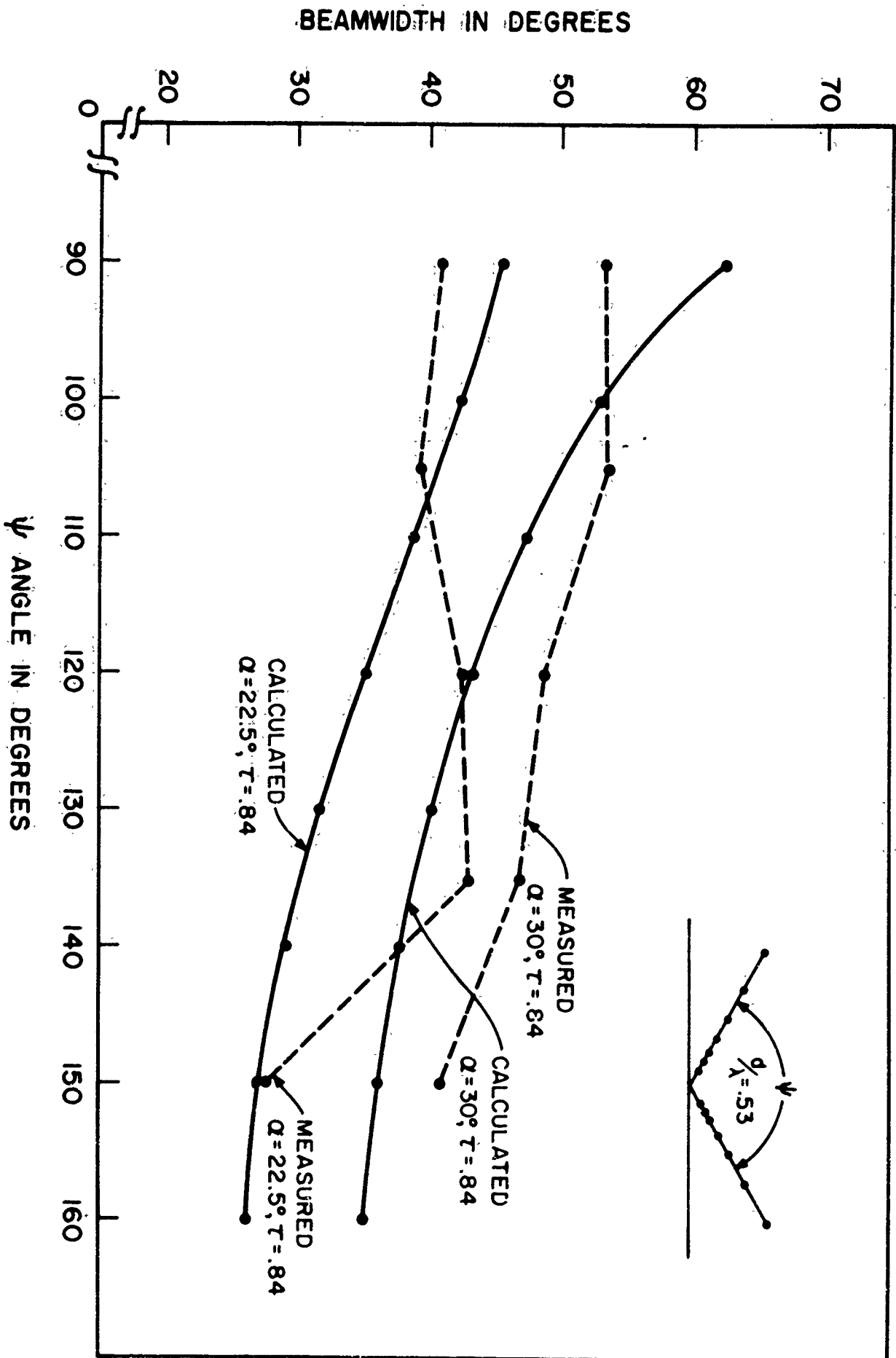


Figure 21. Calculated and measured sum mode beamwidths as a function of ψ angle.

designed and built single element dipole arrays over ground. Some comments on the expected impedance of a single element over ground was made in a report published by Smith Electronics⁶. However, no published data of impedance of a single element over ground was found, and of course, there was no information as to the performance of two elements fed as the structure discussed above.

To get some idea as to how one structure over ground should behave, a few high frequency models were measured in free space as a function of the angle between the planes of the elements. see Figures 22 and 23. Figure 22 shows a plot of input impedance and VSWR of an antenna fed in the sum or difference mode as a function of the angle between the planes of the elements, β , for a structure having a τ ratio of .84 and an α angle of 15° . A single element fed over ground at some angle $\beta/2$ would be inherently in the difference mode due to the 180° current reversal in the image. Figure 23 is the same type of plot except for a structure having a τ ratio of .84 and an α angle of 22.5° . In both cases, the impedance was well behaved in general; and the input VSWR was below 2:1 for a large variation of β angle for both the sum and difference modes of the structure of Figure 22. But, the difference mode VSWR was above 2:1 over the same range of β for the structure of Figure 23. It appears that the mutual coupling between elements is less on the structure having an α angle of 15° , thus, deteriorating the VSWR to a lesser degree as compared to the structure an α angle of 22.5° .

Figure 24 shows the plot of impedance and VSWR as a function $\beta/2$ for a single element over ground. This particular structure had a τ ratio of .84 and an α angle of 17° and was constructed to operate down to a lower frequency. The dashed curve on the plot is for the same single element in free space. If one compares the performance of this structure with the difference mode performance of the structure of Figure 22, it is observed that the shape of the VSWR curve is approximately the same. However, the input impedance curve of this structure is more irregular than the corresponding curve of Figure 22. The variation of input impedance of this structure as a function of angle above ground resembles the variation of the input impedance of a dipole as a function of the height above ground. This seems to be a reasonable comparison, in which an oscillatory type variation occurs near ground

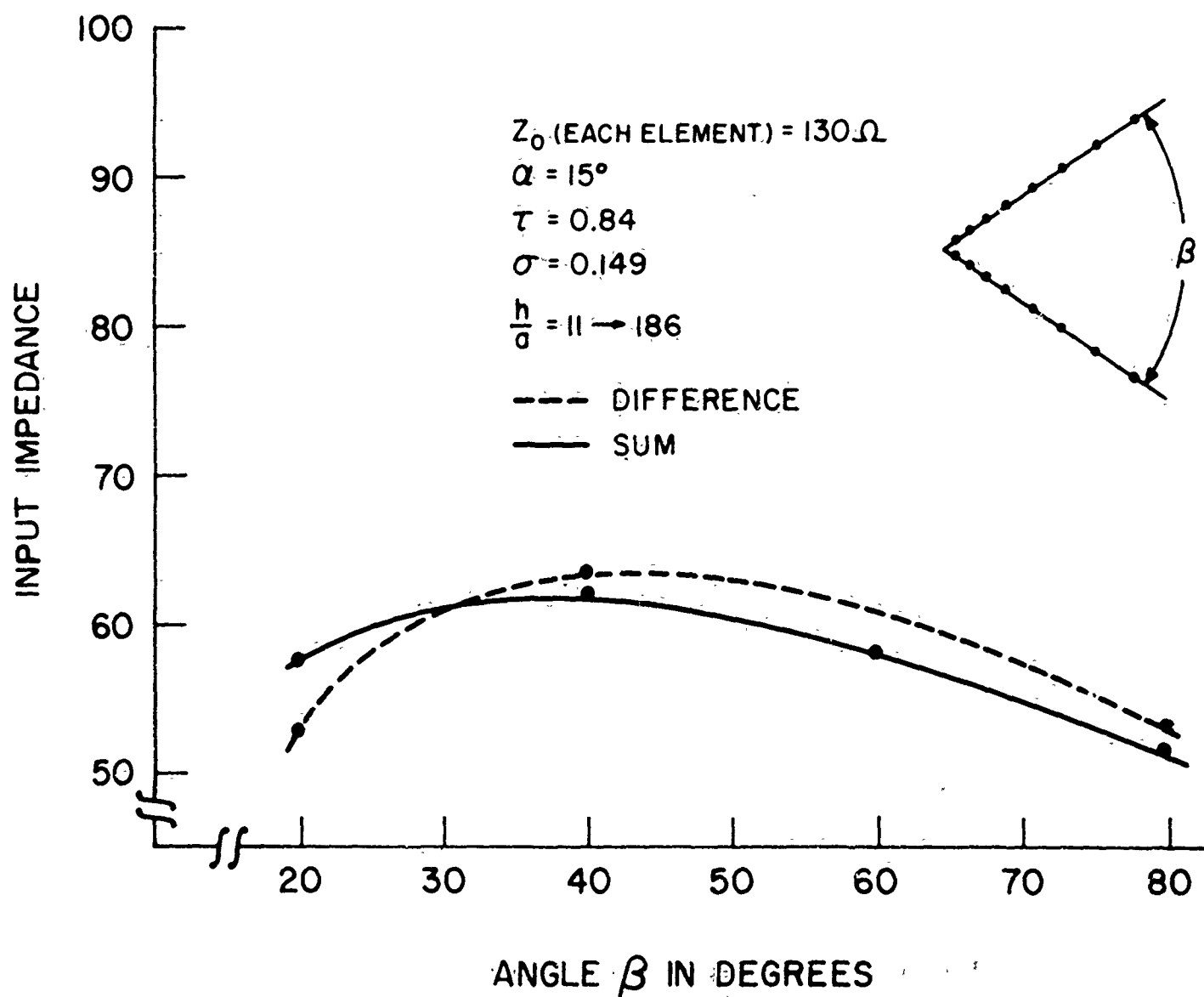
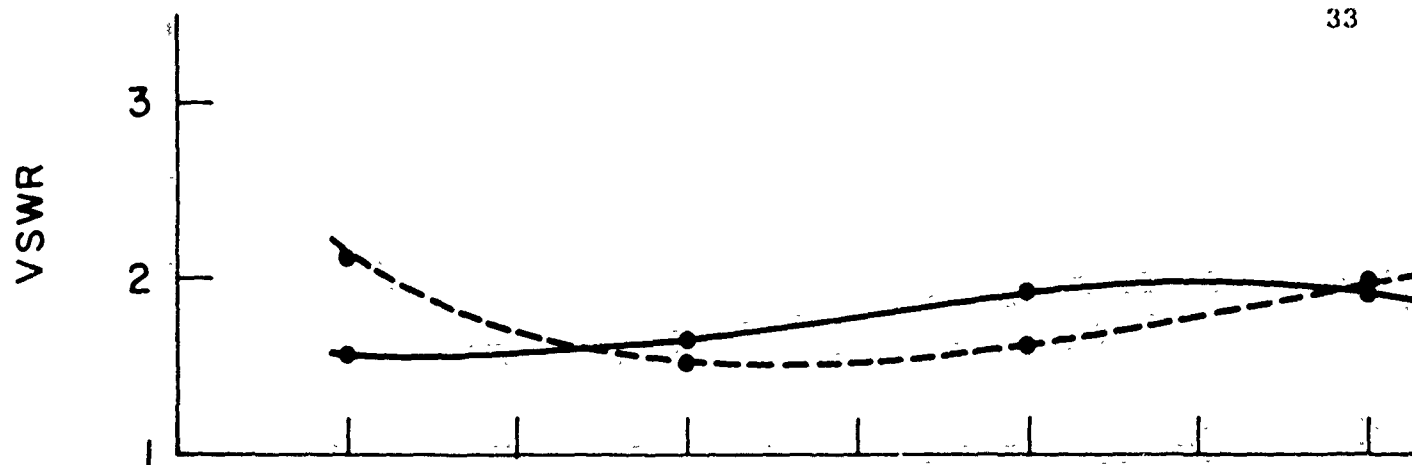


Figure 22. Free space input impedance and VSWR of a two element array connected in a sum or difference mode.

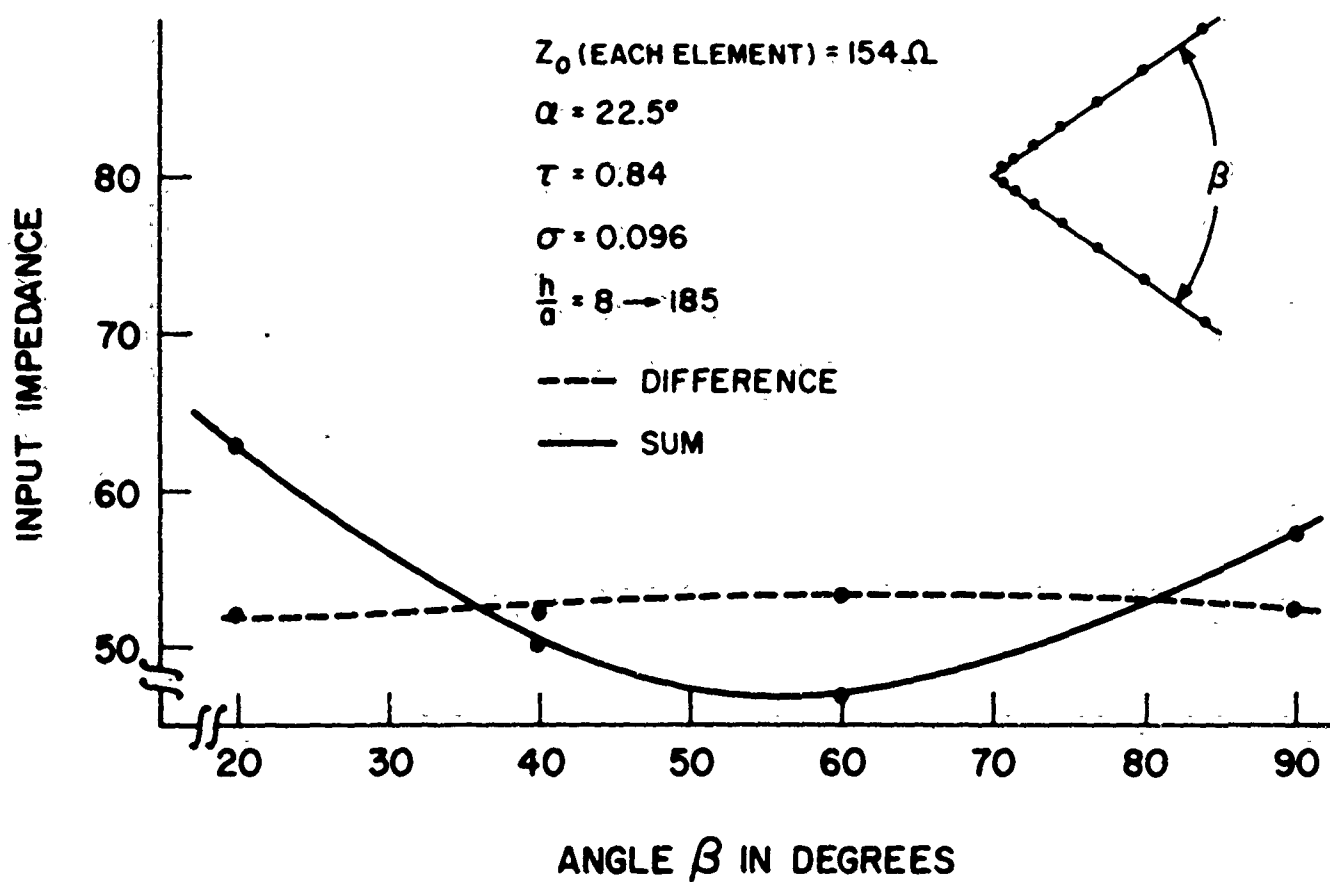
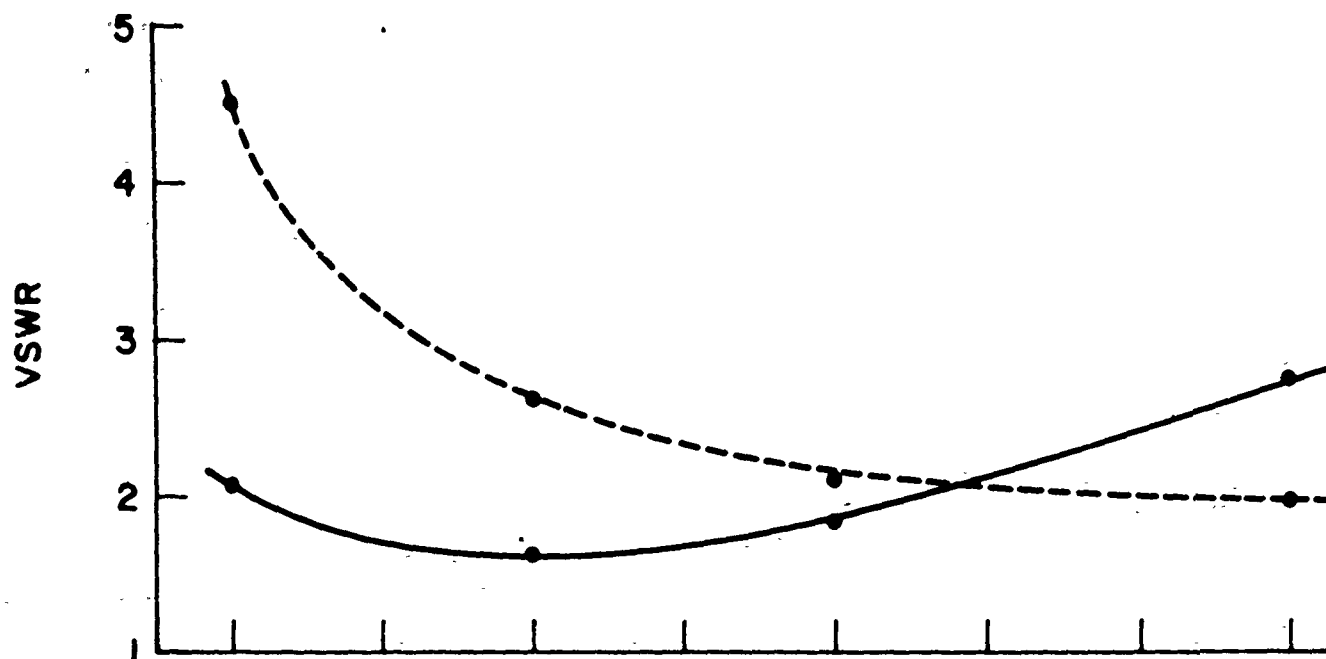


Figure 23. Free space input impedance and VSWR of a two element array connected in a sum or difference mode.

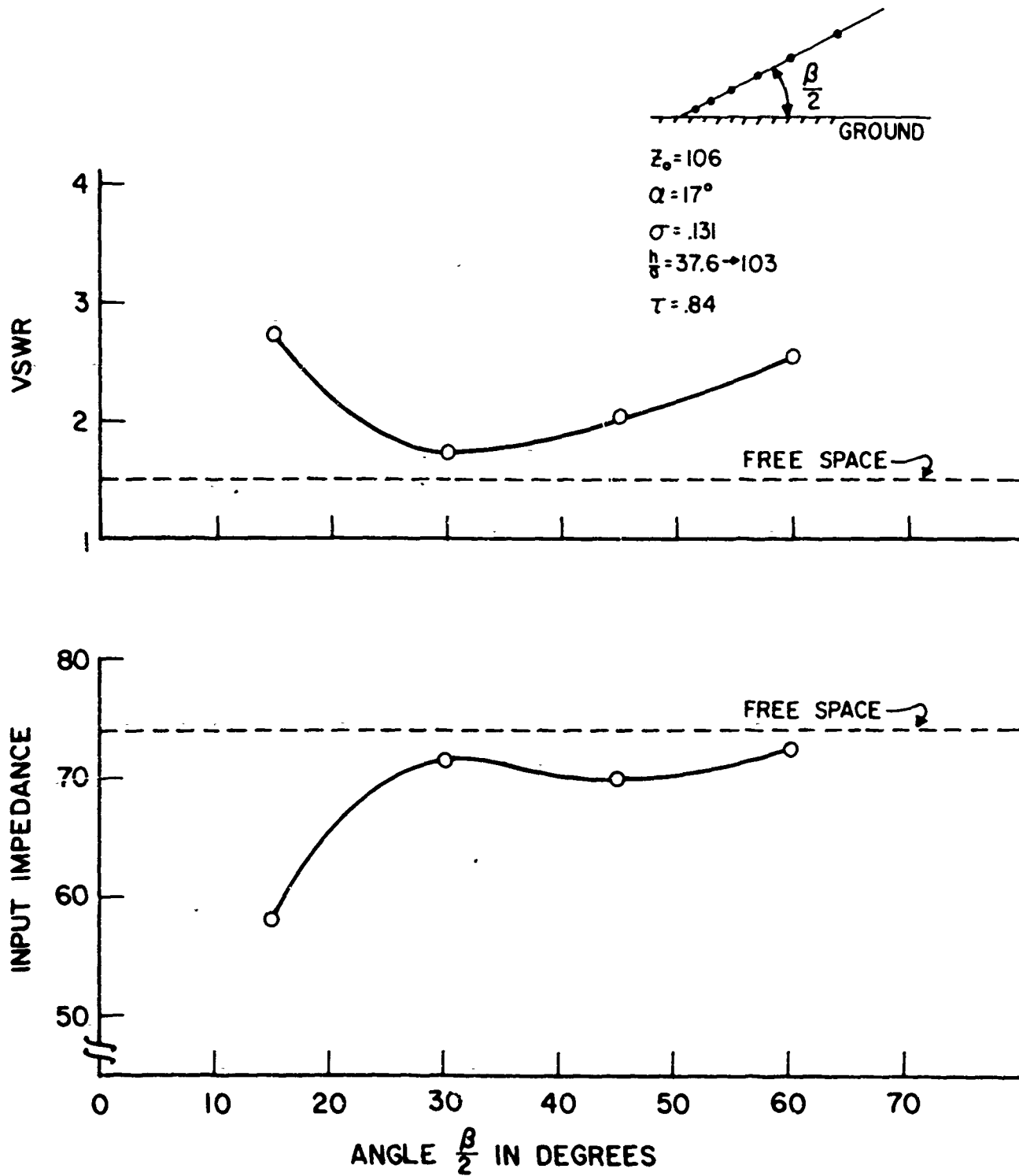


Figure 24. VSWR and input impedance as a function of angle above ground, $\beta/2$, for various α angles.

and the input impedance approaches the free space input impedance as the distance above ground increases.

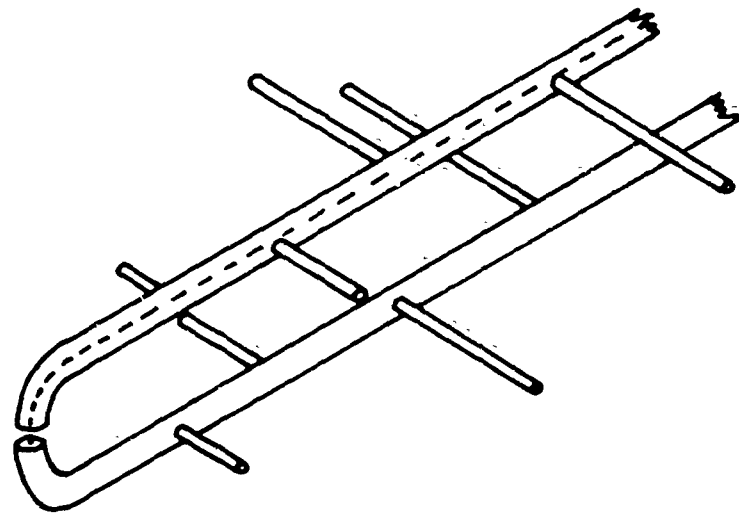
All the dipoles of the models used in obtaining the data in the last three plots were constructed of tubing and/or large wire as indicated by the relatively small h/a ratio of the elements (h is the half length of a dipole and a is the radius of the same dipole). The h/a ratio for these structures was not held constant; that is, the dipoles of the elements in question were not scaled in diameter or the scaling was done in non-periodic steps. The feed transmission lines for these structures consisted of tubing with the feed coaxial line being brought in through one of the tubes (See Figure 25a).

Since the full scale model of this vertical incidence antenna will be constructed for a low frequency of 2 Mc, the dipoles will necessarily be constructed of small cable or wire (less than 1/4 inch in diameter). The h/a ratio of these elements will be very large; for example, if $h = 125$ feet and $a = 1/8$ inch, $h/a = 125 \times 12 \times 8 = 12000$. It is, of course, not feasible to construct a scale model having such a high h/a ratio. In an attempt to be more realistic in the construction of scale models, a model was constructed using wire .025 inches in diameter for the dipoles. The τ ratio of this model was .775, and the model was constructed in such a way that the $\beta/2$ angle could be easily varied. Also, the α angle could be varied with very little reconstruction. The following table gives the low frequency limit, h/a ratio of the antenna for three values of α angle, and a parameter σ (a function of α and τ) that will be defined later.

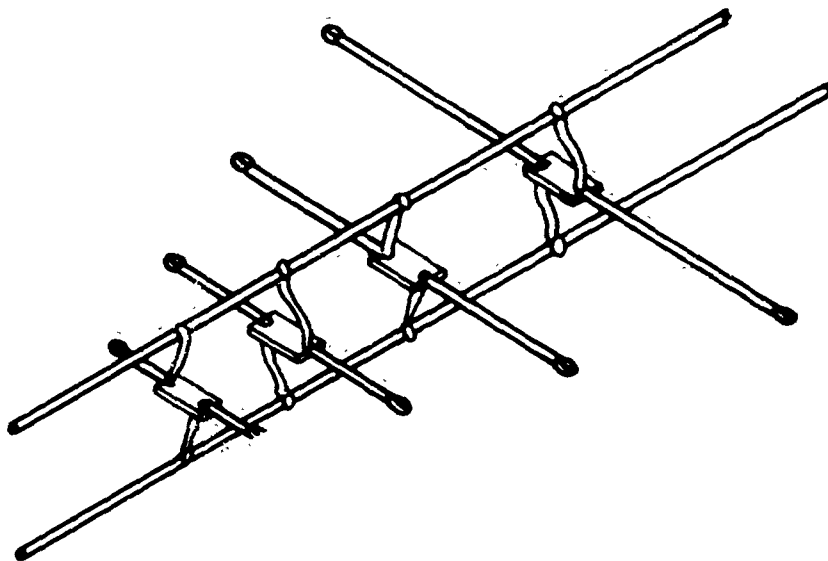
Table II

α	Approximate Low-Frequency Limit	h/a ratio variation	σ
15°	305 Mc	21.8 - 772	.21
22.5°	196 Mc	33.6 - 1193	.136
30°	141 Mc	46.9 - 1660	.097

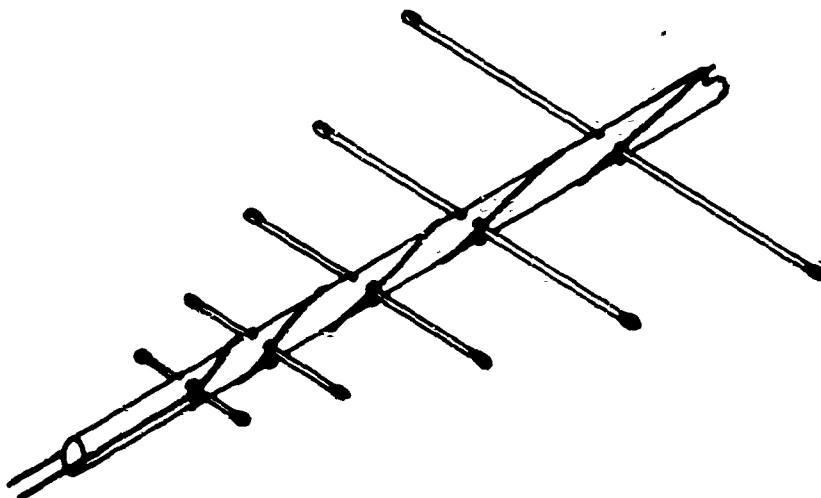
The feed system used for this model was the same as for the previous models, that is, the system as shown in Figure 25a. The impedance of the feeder line was approximately 190 ohms.



(a)



(b)



(c)

Figure 25. Construction techniques used for impedance and pattern models.

The single element input impedance and VSWR were measured as a function of the angle above the ground system, $\beta/2$, for the three α angles. Figure 26 shows a plot of these data. If one compares the 15° α angle plot of Figure 26 with the 17° α angle plot of Figure 24, it is observed that the general performance of the two structures is similar as one would expect. However, the VSWR of the 15° α structure of Figure 26 is slightly higher, and the variation of the input impedance and VSWR with a change in $\beta/2$ angle is more irregular. This is probably due to the high h/a ratio of the second structure as compared to the first. The actual value of input impedance cannot be compared since the first structure had a feeder impedance of 106 ohms and the second structure had a feeder impedance of 190 ohms. As discussed to some length in Carrel's report,² the actual input impedance of a dipole array is a function of the feeder impedance.

Since the last model was designed in such a way that the τ ratio remained constant as the α angle and low frequency limit was varied, another interesting comparison can be made with the calculated data of Carrel's report². Carrel defined a parameter σ which is a function of both α and τ or $\sigma = \lambda/4 (1 - \tau)$. E.g., Figure 27 is a graphic presentation of this comparison.

Presented on this graph are two calculated curves of VSWR as a function of σ for τ ratios of .7 and .8. In both cases the h/a ratio was 177. The measured VSWR curve as a function of σ for a structure having a τ ratio of .775 is as shown. This comparison implies again that a structure with a high h/a ratio is more sensitive to parameter changes than one with a low h/a ratio. This is generally true for a dipole antenna, too.

Since feeder transmission lines made of tubing are not very practical for a full scale model, an attempt was made to replace the tubing with open wire lines as shown in Figure 25b. This meant that the structure must be fed from the front end similar to the first pattern models, that is, by attaching one of the conductors of the open wire line to the center pin of a feed coaxial connector located at the vertex of the structure and attaching the other conductor to the ground near the same point. The measured VSWR of the arrangement was much higher than when the tubing was used. It was felt that perhaps the reason for this high VSWR was that the conductors of the open wire line

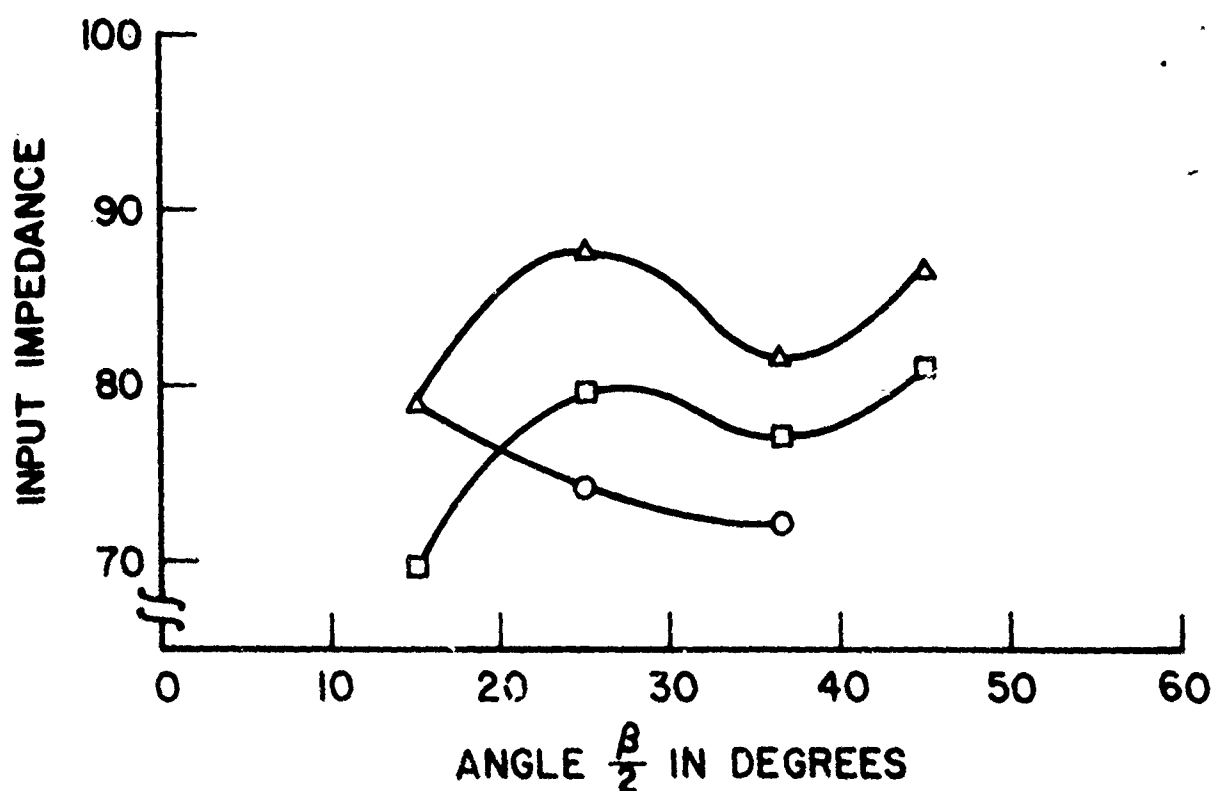
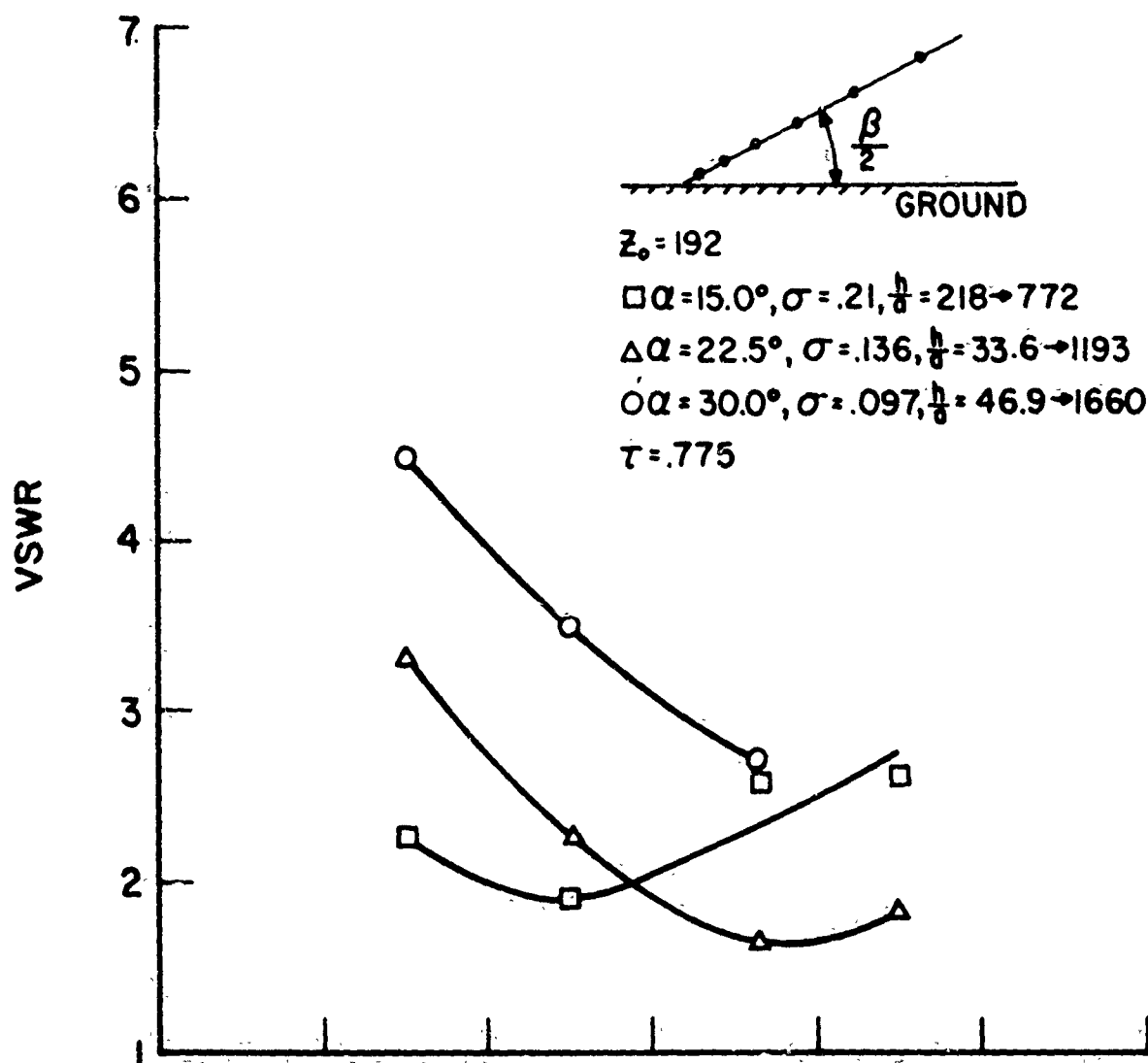


Figure 25. VSWR and input impedance as a function of angle above ground, $\beta/2$, for various α angles.

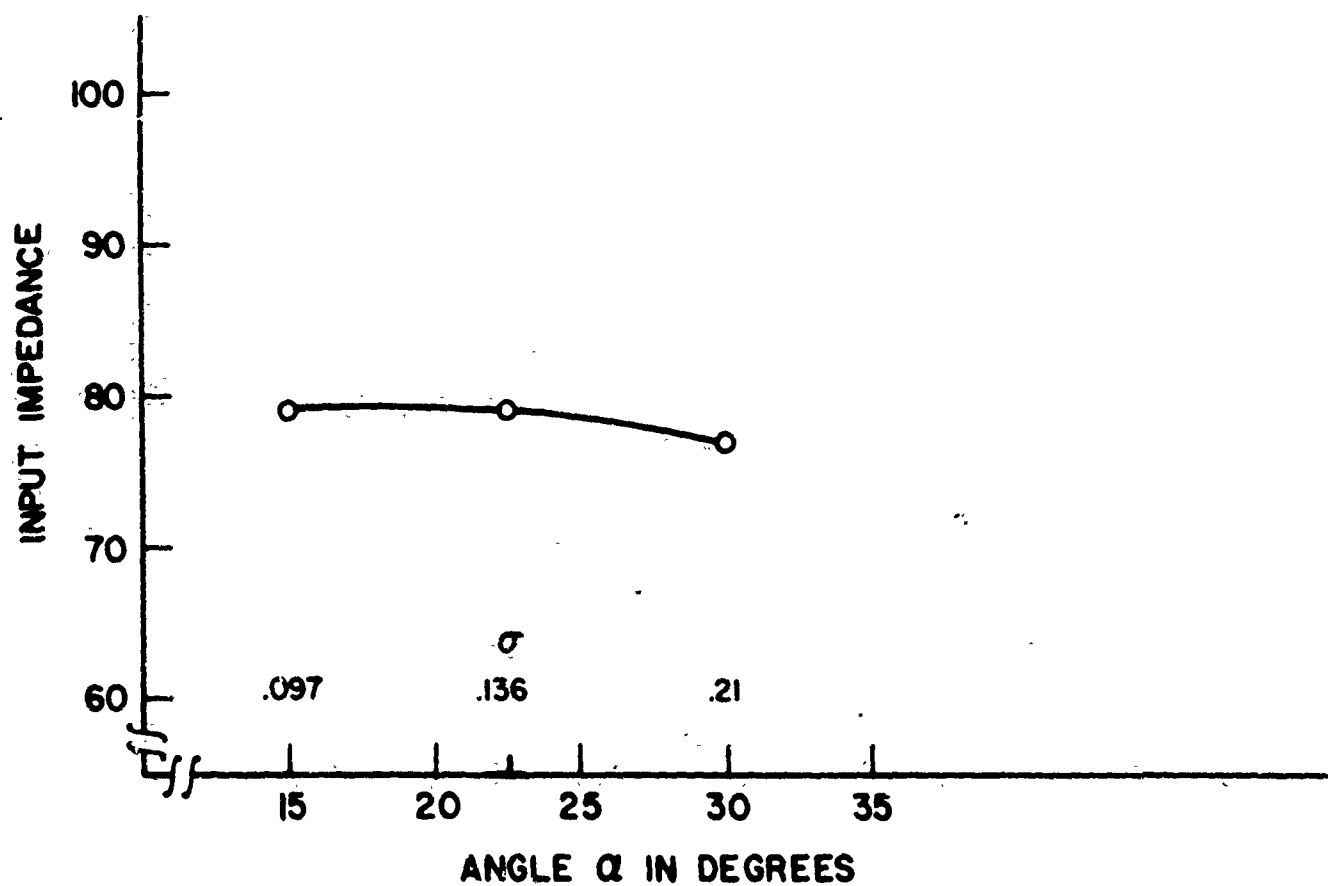
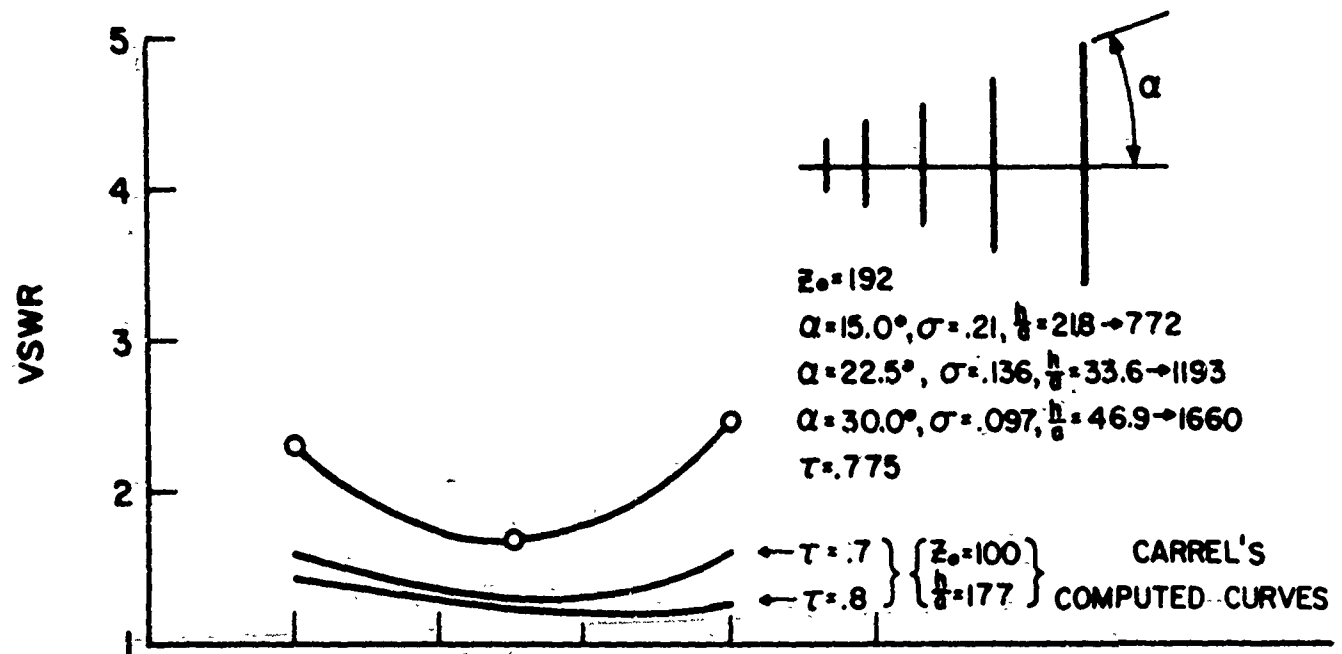


Figure 27. Free space VSWR and input impedance as a function of α angle.

could not be held parallel over the length of the structure.

To provide a solution of this problem and at the same time incorporate additional improvements discovered since building this last wire dipole model, another model was constructed. The dipoles of this latest dipole array model were constructed of wire .008 inches in diameter, in an effort to make this structure even more realistic than the last as far as h/a ratio was concerned. The feederline of this structure consisted of two wires .008 inches in diameter spiraled around a long teflon rod. The objective was to keep these wires as parallel as possible, thus keeping the impedance of the feeder transmission line as uniform as possible. The rod was of the proper diameter to give approximately 300 ohms impedance. Figure 25c shows a sketch of the general coupling arrangement. Here again in the design of this latest structure, means were provided for varying the angle above ground as well as the α angle. The T ratio of this latest structure was .84. Also, this new structure was constructed on a large enough sheet of aluminum that a second structure could be added in the arrangement of Figure 3. Figure 28 is a sketch of one element of this model.

The first step was to measure the VSWR and input impedance of a single element using the feed technique of Figure 6. The Smith Chart plot was rather strange in appearance. The general technique utilized in measuring the impedance of this type structure is to measure approximately five points per period, that is, start at some frequency, say f_1 , and pick four more evenly spaced frequencies over a period such that the last one is equal to $f_1 \tau^{-1}$. For well-behaved log-periodic structure the impedance of f_1 and $f_1 \tau^{-1}$ should be approximately the same. On a Smith Chart plot, a smooth curve drawn through all five points should be approximately a circle. Ordinarily many periods are thusly measured, and the measured VSWR and input impedance are based on the largest circle containing all these points. After measuring this single element over several periods, it was noted that most of the points fell within a very definite area on the Smith Chart; however, several points fell with a more or less random distribution at varying distances from this well-defined area. Checking these "wild points" a second time gave only very minor variation in their location.

Looking closely at a period containing one of these points, it was observed that as the frequency was increased by small increments from a value where the

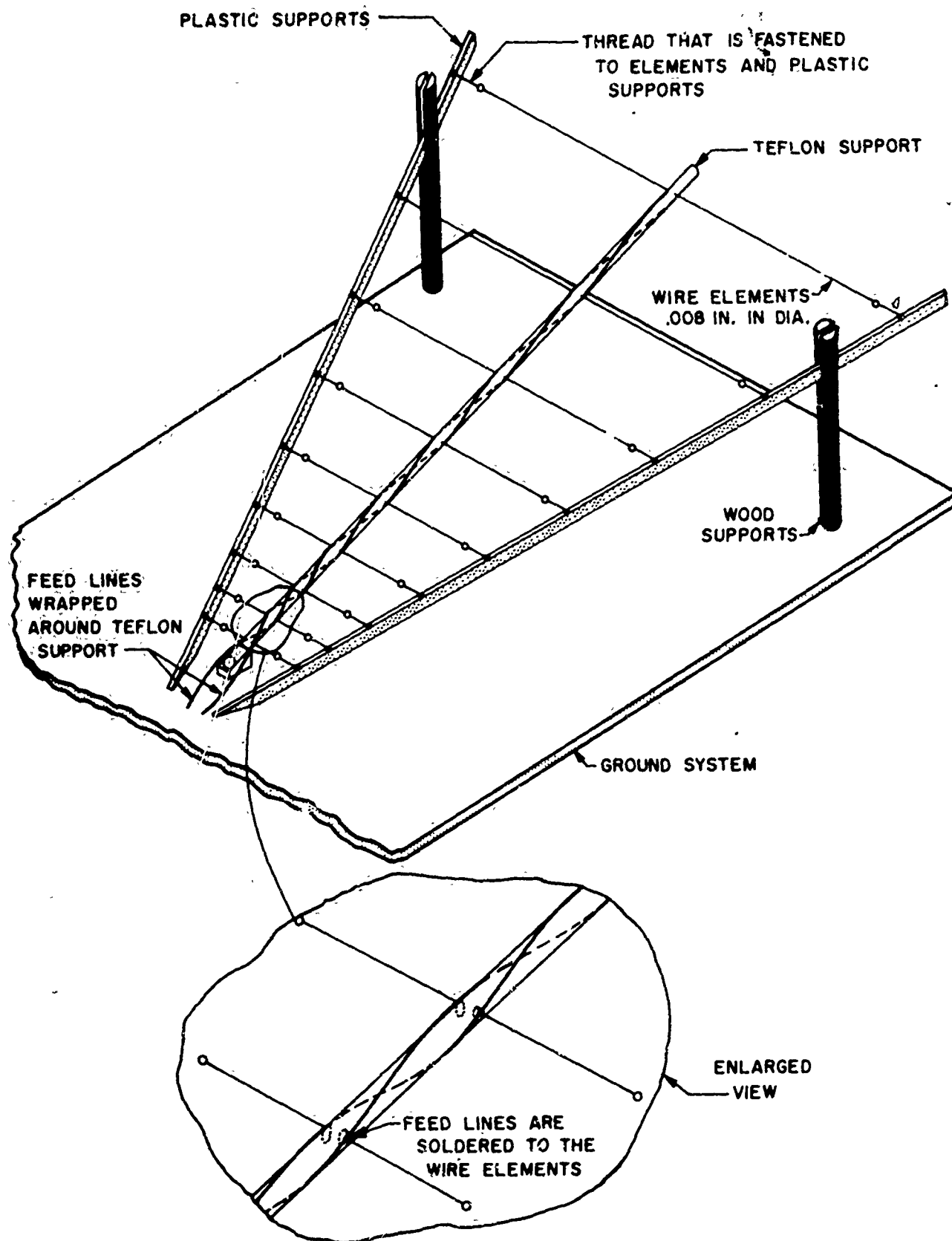


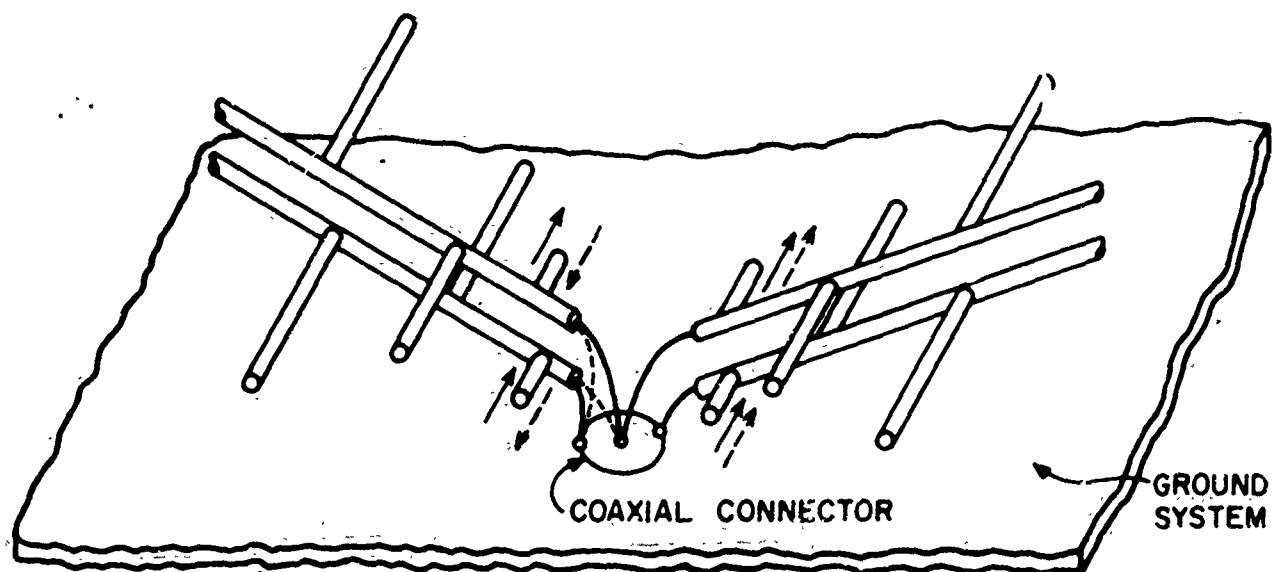
Figure 28. A sketch of the impedance model having the spiral open wire feeder line.

plot was well-behaved to a frequency where one of these "wild points" occurred, the impedance changed very rapidly. In order to determine exactly what was happening the impedance was measured over several of these periods with frequency change increments of 2 Mc in the critical area. It was found that, indeed, the impedance did change smoothly, but rapidly, from the well-behaved area over a very narrow band (for example, a 10 Mc band at approximately 500 Mc). Checking some of the measured periods where this phenomena was not observed at first showed that it occurred between two of the measured points of the original plot. After measuring the antenna carefully over its full frequency range, it was observed that this phenomena occurred once every period.

On checking the radiation patterns of this structure over a couple of periods, it was found that over the band of frequencies where the impedance was erratic the cross polarization became excessive. It was felt that this probably was the reason that excessive cross polarization was observed at some frequencies when the high frequency pattern models were being measured as mentioned in Section 3.

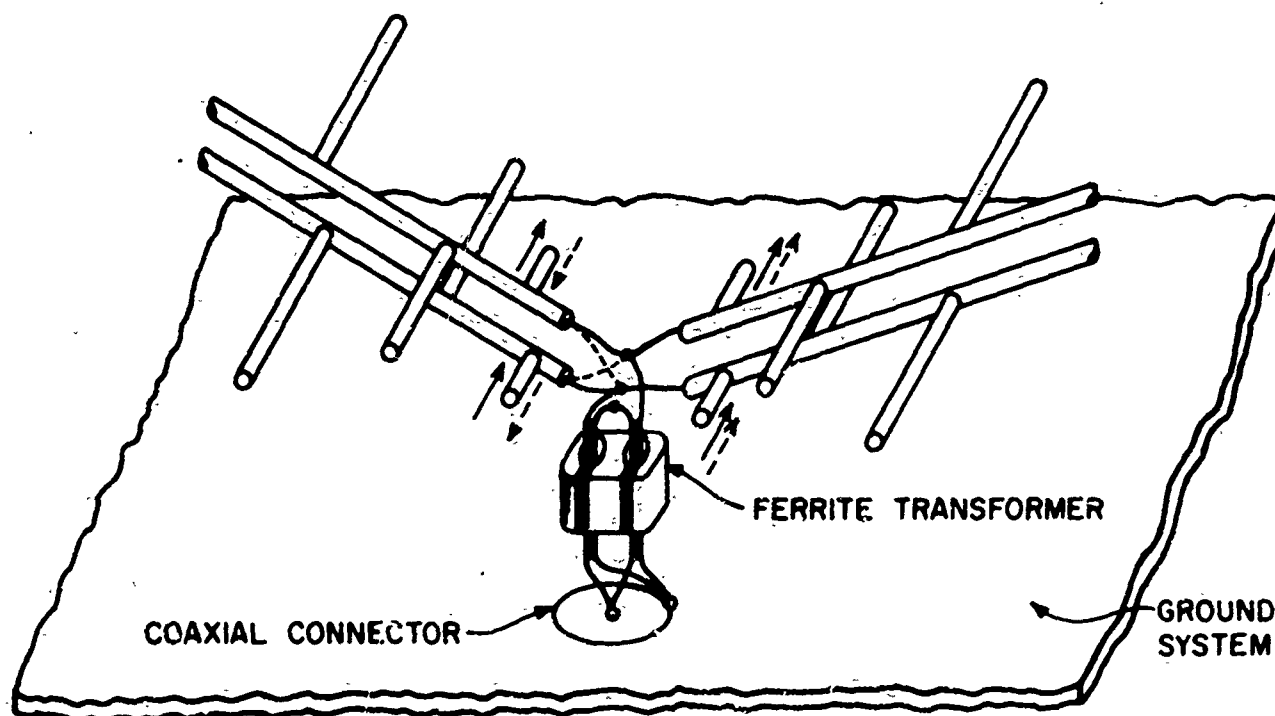
Grounding one of the feeder transmission line conductors and feeding energy to the other, as in Figure 29a, apparently caused the feeder line to radiate over a narrow band of frequencies when the feeder became a certain length in terms of the wavelengths of the energy being fed to the antenna. To prove this was the case, a balun transformer was used to feed the structure over some of the bad periods near the low frequency limit of the antenna (the balun transformer was a bifilar winding on a ferrite core, intended for use in the VHF television frequency range), see Figure 29b. The Smith Chart impedance plot of the antenna impedance through this balun transformer was very well behaved, that is, the plot was a well-defined cluster of points indicative of an almost constant VSWR with respect to the average impedance value. Also, no excessive cross polarization was observed in the radiation patterns.

The problem then was one of finding a balun transformer that would function over a wide frequency range. By experiment, it was found that the first transformer with modifications would operate up to approximately 1000 Mc reasonably well. These modifications consisted of reducing the size of the ferrite core reducing the number of turns, and winding the transformer with



(a)

DOTTED LINES — DIFFERENCE MODE
SOLID LINES — SUM MODE



(b)

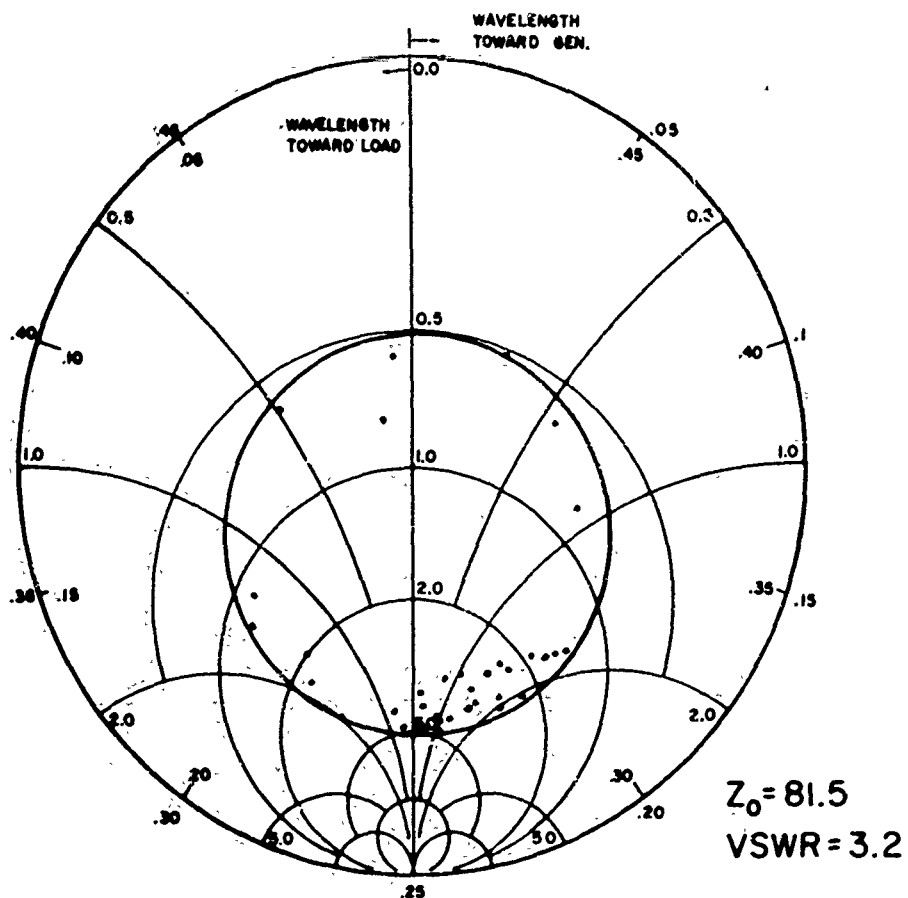
Figure 29. Feed techniques used on low frequency impedance models.

the proper impedance transmission line. Figure 30a is a representative Smith Chart plot of the measured impedance of one element without the transformer; Figure 30b is the measured impedance of the same element measured through the transformer. The average impedance of the element measured through the transformer is much less than that without the transformer since there is approximately a 4:1 impedance transformation in the transformer used. Figure 31 shows a plot of measured data taken on the single log-periodic array element positioned over ground for the parameters as indicated.

At this point it was felt that some meaningful impedance measurements could be made on the two-element vertical incident antenna. So, the second element was constructed and mounted on the same metal plate as the first. Figures 32 and 33 give the measured VSWR and input impedance as a function of $\beta/2$ angle for respectively $\alpha = 30^\circ$ and $\alpha = 22.5^\circ$. It will be observed that data are presented for both the sum and difference modes. The actual impedance levels are not too meaningful since the exact impedance transformation of the transformer is not known. However, the relative levels are felt to be a good indication of how the impedance varies as a function of $\beta/2$. It is interesting to note that the angle corresponding to the optimum VSWR (minimum) is not the same for the sum and difference modes. In the case of $\alpha = 30^\circ$ (Figure 32) the VSWR of the difference mode never gets better than 3.8 to 1 ($\beta/2 \approx 23^\circ$) while the VSWR of the sum mode has a low value of 1.8:1 ($\beta/2 \approx 37^\circ$). For the case of $\alpha = 22.5^\circ$, the optimum VSWR, 1.7:1, for the difference mode occurs at a $\beta/2$ angle of approximately 26° , while the optimum VSWR, 1.9:1, for the sum mode occurs at $\beta/2$ angle of $\beta/2 \approx 36^\circ$.

If one wanted to pick a good compromise value of $\beta/2$ the "cross-over point" of the two curves would be the point to choose. This "cross-over point" occurs at $\beta/2$ angle of approximately 33° for the structure of Figure 33 where the VSWR for both the sum and difference modes is approximately 2:1.

(a)



$\alpha = 22.5$
 $\tau = .84$
 $\beta/2 = 45^\circ$

(b)

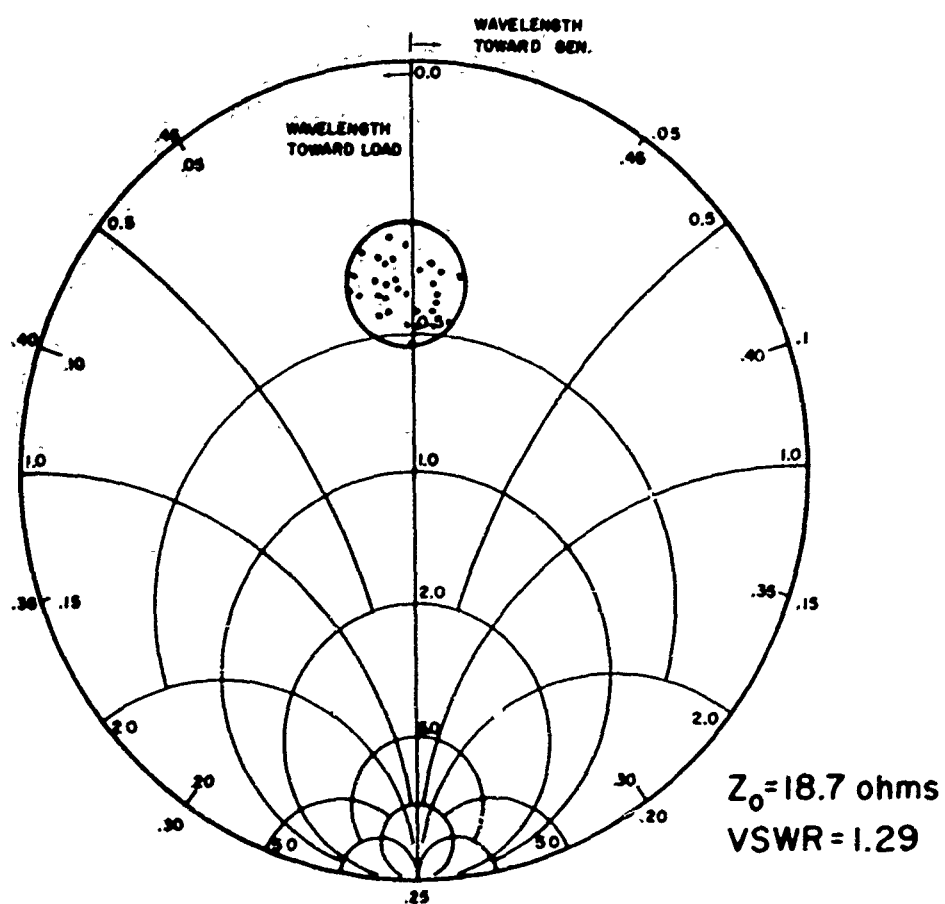


Figure 30. Comparison of the input impedance of a single log-periodic dipole array element over ground, fed at the vertex
 (a) without a transformer (b) with a transformer.

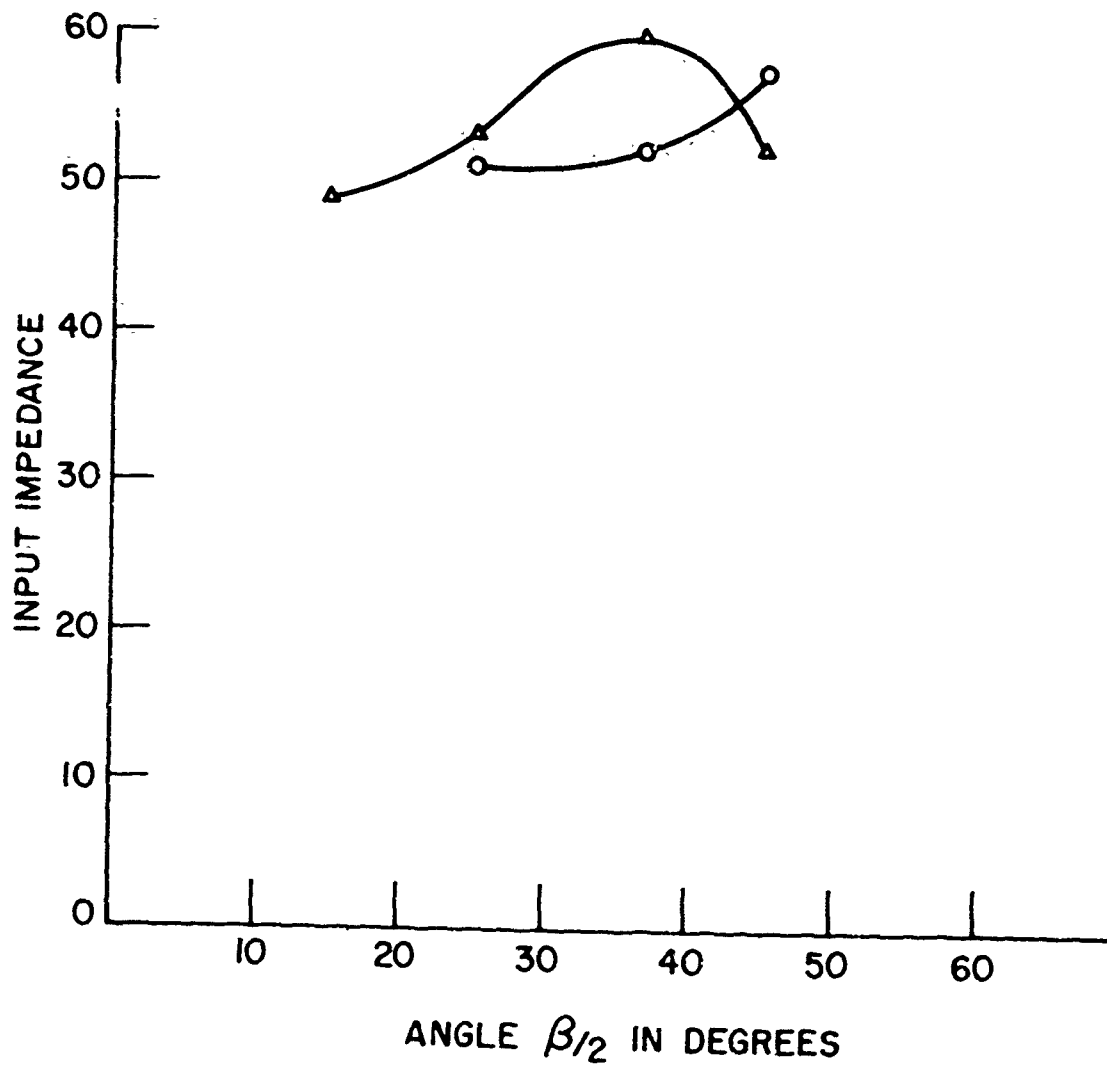
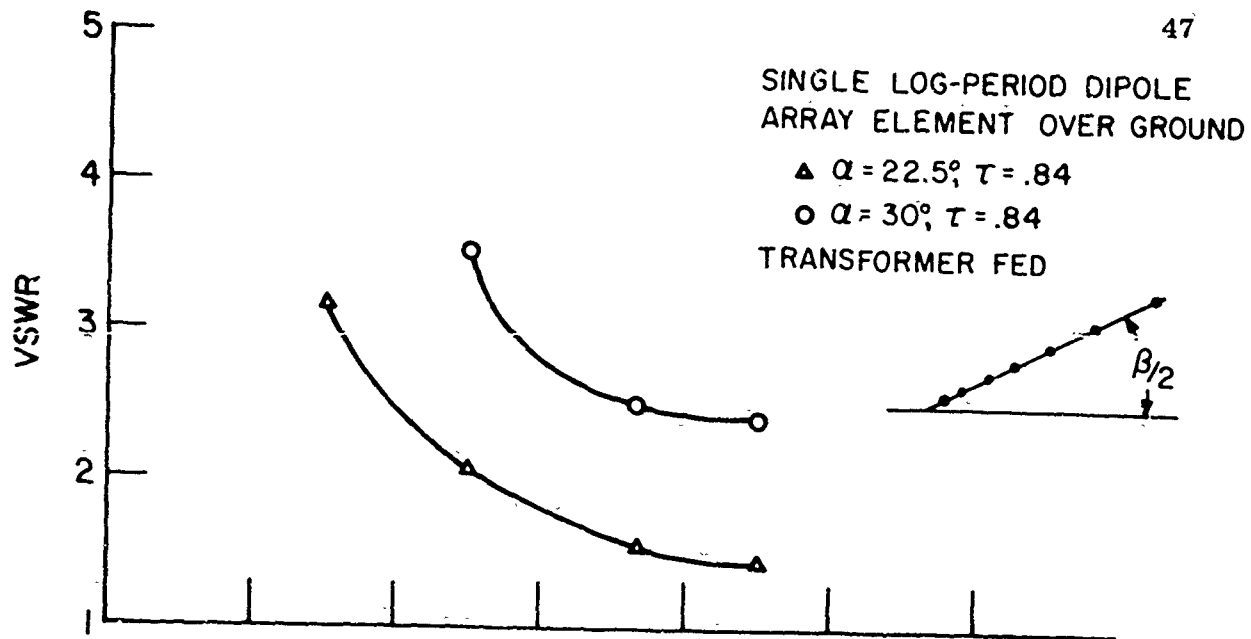


Figure 31. VSWR and input impedance as a function of angle above ground, $\beta/2$, for various α angles.

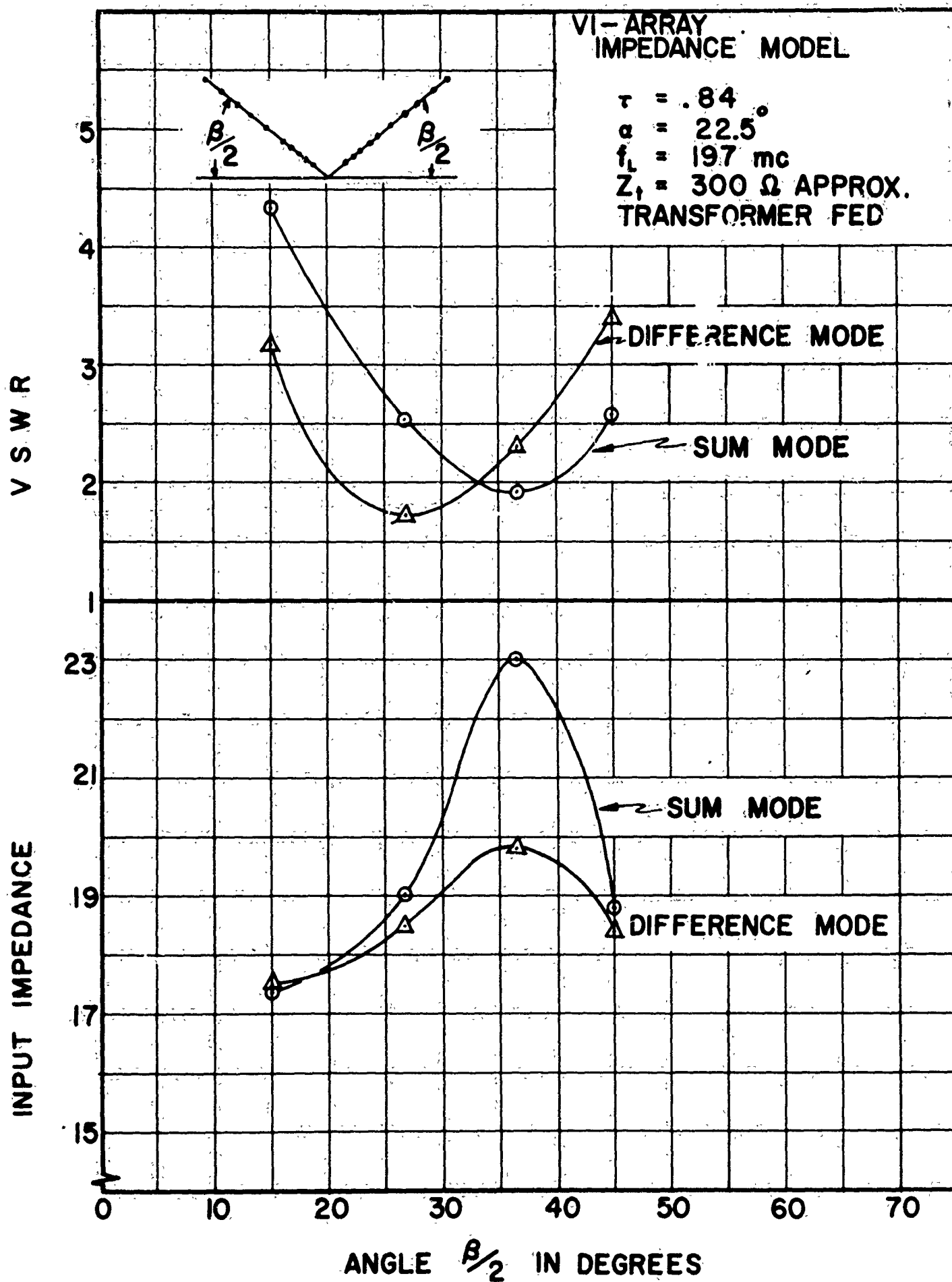


Figure 32. VSWR and input impedance as a function of $\beta/2$ in degrees for sum and difference modes.

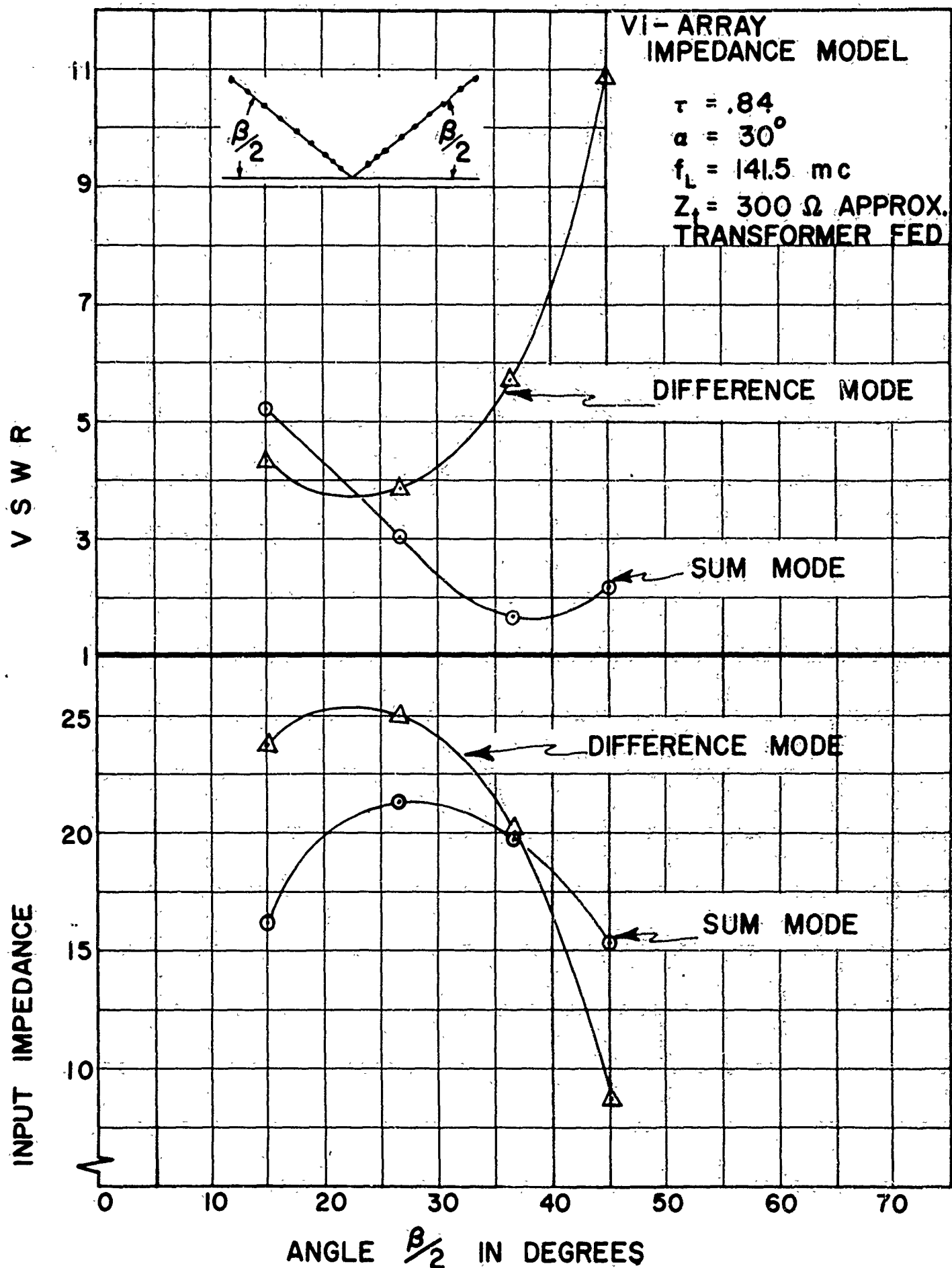


Figure 33. VSWR and input impedance as a function of $b/2$ in degrees for sum and difference modes.

6. Conclusion

The objective of this investigation was to determine the feasibility of designing a wideband, high efficiency vertical incidence antenna capable of producing a single beam centered on the zenith or a split beam with two lobes at an angle θ from the zenith and the null between the lobes centered on the zenith. It is felt that this objective has been realized. The next task was to determine how the performance of a two-element structure is dependent on the many design parameters and to find near optimum design parameters in view of the desired performance and restrictions placed on the choice of design parameter by the physical size of an antenna designed for the 2 to 32 Mc frequency range. It was found that the impedance is very dependent on the parameter variation. If the optimum match for both the sum and difference modes is desired, then a compromise must be made between the optimum match for either the sum or difference modes. Of the antennas thus far tested, it was found that the structure having a τ ratio of .84, a angle of 22.5° and a ψ angle 114° ($\psi = 180^\circ - 2(33^\circ) = 114^\circ$) will give a VSWR of approximately 2:1 for either the sum or the difference mode of operation (see Figure 33). While an optimum VSWR of 1.7 at a $\beta/2$ angle of 23° is possible for the difference mode (at this same $\beta/2$ angle the VSWR for the sum mode is approximately 2.6 to 1). The optimum VSWR for the sum mode was found to be approximately 1.9 to 1 at a $\beta/2$ angle of 36° (the VSWR of the difference mode at this $\beta/2$ angle is approximately 2.3 to 1).

Assuming a ψ angle of 115° , the maxima of the difference lobes would be approximately 32° from the zenith for this same structure. It would appear from the results of this investigation that a compromise in desired pattern performance must be made in order to obtain an antenna with an input VSWR of 2:1 or less. Since the wider α angles produce wider difference lobes and the narrower α angles result in good input VSWR. Instead of desired difference lobe location of 45° from the zenith a more realistic angle would be between 30 and 35° .

The smaller α angles have another deteriorating effect on the performance of the antenna insofar as the sum patterns are concerned. The phase centers of the array elements are farther apart for elements having small α angles and when the planes of the elements are above ground to a point where the

impedance performance is good the phase centers of the elements and their respective images are far enough apart that sidelobes appear on the sum patterns. This is undesirable as far as most radio location applications are concerned.

Also, this investigation has shown that the elements of the two-element array (this will also be true for a four element array) must be fed in a balanced manner. There are available wideband ferrite transformers capable of feeding a balanced antenna from an unbalanced transmission line with the power levels required for the full scale model of the antenna discussed here. These transformers can be purchased to match a wide range of average impedance levels. Thus, the actual average input impedance of the antenna is not important, whereas the variation of the impedance over a period, indicated by the VSWR, is important.

REFERENCE LIST

1. E. C. Hayden and P. E. Mayes, "Supplement No. 1 to the Proposal to Investigate the Possibility of a Very Wide Band Antenna System having Wide Aperture and High Efficiency for Use in Direction Finding and Communication Applications," The Radio Direction Finding Research Laboratory and the Antenna Research Laboratory, Dept. of Electrical Engineering, University of Illinois, Urbana, Illinois, 20 July 1961.
2. R. L. Carrel, "Analysis and Design of the Log-Periodic Dipole Antenna," Antenna Laboratory, Technical Report No. 52, Electrical Engineering Research Laboratory, University of Illinois, Urbana, Illinois, June, 1961.
3. D. G. Berry and M. Bushong, Private Communication Concerning Log-Periodic Monopulse Feeds, Collins Radio Co., Cedar Rapids, Iowa, June 1961.
4. DuHamel and Berry, "Logarithmically Periodic Antenna Arrays," Wescon Convention Record, Pt. I, pp. 161-174, 1958.
5. DuHamel and Ore, "Logarithmically Periodic Antenna Designs," IRE National Convention Record, Part I, pp. 139-151, 1958.
6. Log Periodic Antenna Design Handbook, Smith Electronics, Inc., Cleveland 41, Ohio, October 1961, pp. 4-27.